Running title: Enucleation effects on visuo-tactile connections.

Title: Effects of enucleation on the direct reciprocal corticocortical connections between primary visual and somatosensory cortices of the mouse.

Authors: Ian Omer Massé PhD[1], Gilles Bronchti PhD[2], Denis Boire PhD[2]

Affiliations:

[1]Research Center, Hôpital du Sacré-Cœur de Montréal, 5400 Gouin Ouest Blvd, Montreal, Quebec, Canada, H4J 1C5
[2]Département d'Anatomie, Université du Québec à Trois-Rivières, 3351, des Forges Blvd, C.P. 500, Trois-Rivières, Quebec, Canada, G9A 2W7

Number of pages: 42
Number of figures: 8
Number of tables: 8
Number of equations: 2
Total number of words: 11365
Number of words in abstract: 308

Keywords: Enucleation, cross-modal, corticocortical connections, visuo-haptic interaction.

Corresponding author:

Ian Omer Massé PhD
Centre de recherche
Hôpital du Sacré-Cœur de Montréal
5400, boulevard Gouin Ouest
Montréal, Québec
H4J 1C5

Phone: 514-338-2222 ext 7711
FAX: 514 338-2694
E-mail address: ian.masse.im@gmail.com

Abstract:

Multisensory convergence is present in the cerebral cortex even at the initial stages of processing in the primary and low-level sensory cortices. Direct connections between primary sensory cortices are a particular feature of rodent cortical connectivity. Our previous studies have shown asymmetric projections between the primary visual and somatosensory cortices in mice. Binocular enucleation produces a relative reduction of the projections from the somatosensory cortex to the visual cortex in mice. The purpose of this study is to compare the direct reciprocal cross-modal connections between the primary visual (V1) and somatosensory (S1) cortices in intact and enucleated C57Bl/6 mice, and to determine quantitative differences in the proportion and laminar distribution of neurons and terminals in these projections. CTB labeled neurons were used to estimate the relative importance of projections between V1 and S1, and their laminar distribution used to classify them as feedback, feedforward or lateral projections. The size of axonal swellings was measured and frequency distribution determined for each cortical layer. Axon diameters were also sampled in these connections. Injections in V1 resulted in a reduced proportion of labeled cells in S1 of enucleated mice. There was a relative decrease of the projection from the somatosensory cortex to the visual cortex in enucleated mice due to a greater relative reduction of supragranular layers neurons. Enucleation otherwise had no effect on the connectivity of the somatosensory cortex with other motor and somatosensory cortices. In the projection from the visual to the somatosensory cortex in enucleated mice, the size of axonal swellings was reduced in all layers. Conversely, in the projection from the somatosensory cortex to the visual cortex, some larger swellings appeared in the supragranular layers. This shows pathway and laminar specific changes in cortical circuitry following loss of sensory afferent activity that results in changes in the relationship between visual and somatosensory cortices in the enucleated mice.

Introduction

Multisensory convergence is present in the cerebral cortex even at the initial stages of processing in the primary and low-level sensory cortices. Neurons in primary sensory cortices can respond to inputs from other sensory modalities (Foxe *et al.*, 2000; Schroeder & Foxe, 2005; Ghazanfar & Schroeder, 2006; Bizley *et al.*, 2007; Kayser & Logothetis, 2007; Lakatos *et al.*, 2007; Noesselt *et al.*, 2007; Kayser, 2010; Lewis & Noppeney, 2010; Iurilli *et al.*, 2012; Liang *et al.*, 2013; Rohe & Noppeney, 2016). It is generally believed that this reflects corticocortical feedback projections from higher order association cortices and subcortical structures (Falchier *et al.*, 2002; Clavagnier *et al.*, 2004; Cappe & Barone, 2005; Budinger *et al.*, 2006; Hackett *et al.*, 2007; Budinger *et al.*, 2008; Wang *et al.*, 2008; Campi *et al.*, 2010; Laramee *et al.*, 2011; Charbonneau *et al.*, 2012; Iurilli *et al.*, 2012; Henschke *et al.*, 2015). In contrast to primates (Clavagnier *et al.*, 2004; Cappe & Barone, 2005), and carnivores (Meredith & Lomber, 2017) there are significant direct connections between primary sensory cortices in rodents (Paperna & Malach, 1991; Budinger *et al.*, 2006; Wang & Burkhalter, 2007; Budinger & Scheich, 2009; Campi *et al.*, 2010; Charbonneau *et al.*, 2012; Iurilli *et al.*, 2012; Sieben *et al.*, 2013; Zingg *et al.*, 2014; Henschke *et al.*, 2015; Massé *et al.*, 2016; see also Meredith & Lomber, 2017). Therefore, direct interactions between primary sensory cortices are a particular feature of the rodent cortex.

We have previously shown asymmetric reciprocal connections between the primary visual and somatosensory barrel field in the mouse (Massé *et al.*, 2016). The projection from V1 to the barrel field originates from both supra- and infragranular layer neurons whereas the projection from the barrel field to V1, mostly from infragranular layer neurons in both mice

and gerbils (Henschke *et al.*, 2015; Massé *et al.*, 2016). Laminar origin of cortical projections is an important structural feature of corticocortical projections. In primates and rodents, feedforward projections originate mainly from supragranular layers neurons and feedback projections, from infragranular layers neurons (Rockland & Pandya, 1979; Coogan & Burkhalter, 1990; Felleman & Van Essen, 1991; Coogan & Burkhalter, 1993). Therefore, the projection from V1 to S1 has morphological features of a lateral connection whereas the projection from S1 to V1, features of a feedback projection. Moreover, there is a greater incidence of larger axonal swellings and larger axon calibers in the projection from V1 to the somatosensory barrel field, suggesting a greater incidence of Class 1 synapses in this projection. (Covic & Sherman, 2011; De Pasquale & Sherman, 2011; Petrof & Sherman, 2013). Comparison of the structure of reciprocal cortical projections is instrumental in determining the position of the primary sensory areas in the cortical network (Coogan & Burkhalter, 1990; Felleman & Van Essen, 1991; Coogan & Burkhalter, 1993; Barone *et al.*, 2000; Hilgetag *et al.*, 2000; Barone *et al.*, 2013; Markov *et al.*, 2014). Asymmetries in the reciprocal projections between primary sensory areas could support the proposal that primary sensory cortices have different connectivity patterns in the neocortical network.

Corticocortical connections generally develop by an initial overproduction of projections followed by a selective elimination of the exuberant projections guided by afferent sensory activity (Innocenti & Price, 2005; Price et al., 2006) resulting in the mature pattern of cortical connectivity. In primates and rodents, there is a significant reduction in the number of supragranular layers neurons that establish feedback projections to V1 whereas infragranular layers connections are established much earlier in development (Coogan &

Burkhalter, 1988; Batardiere *et al.*, 2002; Berezovskii *et al.*, 2011; Khalil & Levitt, 2014). Therefore, feedback cortical pathways undergoe more extensive sensory dependant postnatal remodeling than cortical feedforward pathways.

Studies in deaf ferrets (Allman *et al.*, 2009; Meredith & Allman, 2012) and cats (Barone *et al.*, 2013; Kok *et al.*, 2014; Chabot *et al.*, 2015; Butler *et al.*, 2016a; b; Meredith *et al.*, 2016) show that connectivity patterns are generally preserved in deaf animals. Mice bilaterally enucleated at birth and intact mice have the same complement of cortical and subcortical projections. However, neonatal bilateral enucleation reduced the number of neurons of the somatosensory cortex projecting to the primary visual cortex in mice (Charbonneau *et al.*, 2012). Moreover, corticocortical connections were not modified in $Gnat^{-/-}$ mice in which only cone mediated vision remains intact (Larsen *et al.*, 2009). Conversely, early sustained sensory deprivation enhanced direct corticocortical projections between primary sensory cortices were reported in subadult (P28) gerbils (Henschke *et al.*, 2017). Corticocortical connections are expanded in enucleated opossums (Karlen *et al.*, 2006), suggesting that perhaps in marsupials the removal of the eyes at a very early stage of development compared to rodents, might alter cortical connections to a greater extent.

In the developing primates, the later maturation of feedback projections does not change the relative connectivity patterns of visual cortical areas (Batardiere *et al.*, 2002). However, in visual areas of monkeys enucleated in the prenatal period, there is an increase in the relative number of supragranular layers feedback projecting neurons, altering the structure of extrastriate visual cortices. (Magrou *et al.*, 2017). Similarly, after early and sustained sensory deprivation in gerbils, many projections between primary sensory cortices maintained more numerous supragranular layers projection neurons, indicating that they

retain a less mature laminar feedforward-like pattern (Henschke *et al.*, 2017) and that afferent sensory activity is required for the establishment of the normal connectivity patterns. The quantitative effects of neonatal bilateral enucleation on the reciprocal corticocortical connections between the primary visual and somatosensory cortices were studied here in adult mice to better understand how afferent sensory activity affects their reciprocal asymmetric connectivity and relative structure.

Experimental Procedure

Animals were treated in accordance with the regulations of the Canadian Council for the Protection of Animals and the study was approved by the Animal Care committee of the Université du Québec à Trois-Rivières. C57Bl/6J mice (n=40) (Charles River, Montreal, QC, Canada) from our colonies were used. Neuronal tracers were injected in intact C57Bl/6J mice (n=20) and neonatally enucleated C57Bl/6J mice (n=20). All animals were kept under a light/dark cycle of 14/10 hours and were adults (60 days) when sacrificed.

Neonatal enucleation

Bilateral enucleations of C57Bl/6J mouse pups were performed within 24 h following birth under deep anesthesia by hypothermia. The palpebral fissure was opened with a scalpel, the eyeball was gently pulled out and the optic nerve was sectioned. Ocular orbits were filled with Gelfoam (Upjohn, Kalamazoo, MI, USA) and newborns were warmed until complete awakening before being returned to their home cage.

Tracing procedures

All animals were adults (60 days) when the cortical tracer injections were performed. Surgical anesthesia was achieved and maintained with inhalation of 1.5-2.5% isoflurane and vital signs were monitored throughout the procedures. The animals were mounted on a stereotaxic apparatus. Mice were protected from ocular dryness by applying ophthalmic ointment (Polysporin; Pfizer, Toronto, ON, Canada). A scalp incision was made along the midline to expose the skull. For injections in the primary visual cortex (V1), a small craniotomy was performed 3.7 mm caudal and 2.5 mm lateral to Bregma or, for injections in the barrel field of the primary somatosensory cortex (S1BF), 1.5 mm caudal to Bregma

and 2.9 mm from the midline. The dura was incised and a glass micropipette filled with a solution of the B-fragment of cholera toxin (CTB) or biotinylated dextran amine (BDA) was inserted into the cortex. Retrograde and anterograde neuronal tracing was achieved with iontophoretic injections of 1% solution of CTB and of a 10% solution of high molecular weight BDA (10 kDa) (Molecular Probes, Cedarlane Laboratories, Ontario, Canada) respectively in phosphate-buffered saline (PBS) through glass micropipettes (20 µm tip diameter). A total of 40 mice were utilized for this study. For each tracer, injections were performed into V1 of 5 intact and 5 enucleated mice and into S1BF also in 5 intact and 5 enucleated mice. Cases details are summarized in Table 1. A 1.5 µA positive current with a 7-s duty cycle was applied for 10 min, starting at a depth of 500 µm and ending at 100 µm from the pial surface, 2 min at each 100 µm. The mice were kept warm until they recovered from anesthesia and postoperative pain was managed with buprenorphine (Temgesic, Schering-Plough, Hertfordshire, UK; i.p.; 0.009 mg/kg) injected before anesthesia was induced.

After a 2-day survival period for CTB or 7-day survival period for BDA injected cases, mice received an intraperitoneal injection of 120 mg/kg sodium pentobarbital (Euthanyl; Bimeda-MTC, Cambridge, ON, Canada) and were perfused through the heart with PBS (pH 7.4) followed by phosphate-buffered 4% paraformaldehyde. Brains were harvested, postfixed for 1-2 hours, cryoprotected with 30% sucrose and frozen prior to sectioning and CTB or BDA processing.

Serial 50-µm-thick coronal sections were taken using a freezing microtome. One series was processed for CTB immunohistochemistry and the other was mounted on slides and stained with cresyl violet to identify the cortical areas and layers. Sections processed for

BDA histochemistry were counterstained with bisbenzimide to identify the cortical areas and layers.

To visualize CTB labeled neurons, free-floating sections were treated for 45 min with 0.15% H_2O_2 and 70% methanol to quench endogenous peroxidase and thoroughly rinsed in 0.05 M Tris-HCl-buffered 0.9% saline solution (TBS, pH 8.0) containing 0.5% Triton X-100 (TBS-Tx). Sections were then incubated in 2% normal donkey serum (NDS) for 2 hours and transferred to a solution of primary antibody (goat polyclonal anti-CTB 1:4 000; Molecular Probes) with 1% NDS in PBS-Tx for 2 days at 4°C. Subsequently, sections were rinsed in PBS-Tx and incubated in a secondary antibody (biotinylated donkey anti-goat; 1:500; Molecular Probes) solution with 1% NDS in PBS-Tx for 2 hours at room temperature. Following further rinsing, the sections were then incubated for 90 min in an avidin-biotin complex solution (Elite Vectastain, Vector Laboratories, PK4000 Standard kit) in TBS-Tx (pH 8.0), rinsed in TBS, and then incubated in a 0.015% ’3-diaminobenzidine (DBA) solution. Labeled neurons were revealed by the addition of 0.005% H_2O_2. Sections were washed and mounted on gelatin-subbed slides, air-dried, dehydrated and cover-slipped with Permount mounting media (Fisher Scientific, Ottawa, ON, Canada).

For BDA staining, after quenching endogenous peroxidase, sections were incubated for 90 min in an avidin-biotin complex solution (ABC Vectastain Elite), washed and BDA was revealed using nickel-intensified DAB (Sigma-Aldrich, St-Louis, MO, USA) as a chromogen. Sections were pre-incubated for 30 min in Tris-buffered (TB) (0.05 M) 0.4%, nickel ammonium sulfate (pH 8.0), followed by 10 min in TB-nickel ammonium

containing 0.015% DAB and 0.005% H_2O_2. Sections were dehydrated in ethanol, cleared in xylenes and cover-slipped with Eukitt mounting media.

Charting of retrogradely labeled neurons

All CTB retrogradely labeled neurons on one of every two sections were plotted using an Olympus BX51WI microscope (20 x 0.75 NA objective) equipped with a three-axis computer-controlled stepping motor system coupled to a personal computer and to a color Optronix CCD camera and driven by the Neurolucida software (MBF Biosciences, Williston, VT, USA). In the cases injected in the visual cortex, labeled neurons were charted in areas of S1, S1BF, V2M and V2L. In the cases injected in the somatosensory cortex, labeled neurons were charted in areas. M1, M2, S2 and V1.

The whole primary and secondary somatosensory, motor and visual cortices were systematically sampled on sections spaced 200 µm apart. Cortical areas were delineated at lower magnification (4 X, 0.16 NA objective) on adjacent Nissl-stained sections. Borders between cortical areas were delineated according to the cytoarchitectonic descriptions provided by (Caviness, 1975) and the mouse brain atlas of (Franklin & Paxinos, 2008). Contours of each cortical area in which retrogradely labeled cells were located were traced with Neurolucida and the limits of each cortical layer were traced. These contours were superimposed on the images of CTB-reacted sections and resized for shrinkage differences between the Nissl and CTB sections. This allowed plotted neurons in each cortical area to be assigned to supragranular, granular or infragranular layers for the calculation of layer indices. These indices provide a quantitative assessment of the laminar distribution of retrogradely labeled neurons and are instrumental in the classification of corticocortical

feedback, feedforward and lateral connections (Felleman & Van Essen, 1991). Layer indices (L) were calculated using the contrast formula:

$$L = (S - I)/(S + I)$$

where S and I are the numbers of labeled neurons in supragranular and infragranular layers respectively (Cappe & Barone, 2005; Budinger *et al.*, 2006; Budinger *et al.*, 2008; Budinger & Scheich, 2009). The indices range between -1 and 1. Negative values less than -0.1 indicate feedback connections mostly originating in infragranular layers and positive values indicate greater than +0.1 indicate feedforward connections mostly originating in supragranular layers. Values between -0.1 and +0.1 indicate lateral connections (Budinger *et al.*, 2006). This rule of thumb derives from previous studies of the anatomical definition of cortical connections that proposed that projections with more than 55% of neurons in the supragranular layer to be feedforward and connections with more than 55% of neurons in infragranular layer to be feedback projections thus defining the boundaries for these layer indices (Hilgetag & Grant, 2000; Cappe & Barone, 2005; Barone *et al.*, 2013). All photomicrographs were cropped and luminosity and contrast were adjusted with Adobe Photoshop software.

Stereological sampling of laminar distribution of axonal swellings

In order to provide an unbiased frequency distribution of axonal swellings size in each cortical layer for the projection from V1 to the S1 barrel field and the reciprocal projection from the S1 barrel field to V1, a stereological systematic random sampling of these projection fields was performed using the Stereo Investigator software (MBF Bioscience). Axonal swellings were identified as localized *en passant* varicosities that appeared thicker

than the adjacent axonal segment or terminal axonal swellings. They appeared more darkly stained, as the density of the reaction product chromogen seems greater than in the thinner flanking axonal segments.

Projection fields in which anterograde labeling was observed were sampled using the optical fractionator workflow (in Stereo Investigator) on approximately 10 equidistant sections covering the full rostrocaudal range of the projection, except for the fourth intact case injected with BDA in V1 in which the projection extended to only 5 sections. On each section, polygonal contours were traced at low magnification (4X or 10X) around the projection field. The borders between cortical layers were delineated at higher magnifications in order to obtain non-overlapping and exactly contiguous borders between adjacent layers The stereological sampling and axonal size measurements were then performed at higher magnification (100X, 1.4 NA objective) in no less than 100 square disectors of 20 μm side length and 15 μm height, evenly distributed at the intersections of an 80x80 μm sampling spacing grid for each cortical layer for each case (see Tables 4-7). The maximum diameter of each axonal swelling included in the stereological sampling was measured using the diameter tool in Neurolucida.

This optical fractionator sampling strategy allowed for the estimation of the total number of swellings in each cortical layer. The total numbers of swellings (N) were calculated by the following equation (West *et al.*, 1991):

$$\mathrm{N} = \Sigma\,\mathrm{Q} \times \mathrm{ssf}^{-1} \times \mathrm{asf}^{-1} \times \mathrm{tsf}^{-1}$$

where ΣQ is the total number of swellings counted within the disectors, ssf is the section sampling fraction (number of sampled sections over the total number of sections on which

the terminal projection field appears), asf is the area sampling fraction (ratio of the frame area/the total area of the reference space on the section) and tsf is the thickness-sampling fraction (disector height/section thickness). Product of ssf, asf and tsf is the overall sampling faction (see Tables 4-7). Coefficients of error (CEs) were calculated according to the procedure described by (West & Gundersen, 1990), in order to determine whether the sampling effort was sufficient. It is widely accepted as a rule of thumb that CEs below 0.1 are indicative of a sufficient sampling. The main objective of this stereological sampling was not to determine the total number of swellings that are labeled for each injection, as this number is a function of the injection size, but to obtain unbiased estimates of laminar and size distributions.

Sampling of axonal diameters

In order to compare the caliber of the axonal population entering the cortical areas V1 and the somatosensory barrel field between the intact and enucleated cases, the initial diameter of the axons as they leave the white matter to enter the cortical grey layers of the target was calculated. Axonal diameter changes over short distances and a single point measurement of the axonal diameter was not deemed adequate. To take this into account and to obtain an unbiased estimate of the axons diameters, a weighted average of diameter for the initial 25 μm of each axon was calculated.

The Neurolucida software encodes reconstructions of traced axons as a succession of small segments. Each segment is attributed coordinates in three-dimensional space, a length and a diameter. These segments correspond to the interval between two mouse clicks as the observer traces the axons. These clicks were done to record changes in direction and/or

diameter of the axons. The axon diameter as it enters the cortical grey matter was estimated by the average diameter over the first 25 μm of the axon tracings from their point of entry into the cortical grey matter, weighted by the length of the segments recorded over this distance.

The sampling of the measured axons was performed on the same sections that were used for the stereological sampling of axonal swellings (see Tables 4-7) to ensure that axons were systematically and randomly selected. Axons were selected as they crossed the line between the white and grey matter. The total length of this line for each case and the number of sampled sections are given in Table 8.

Statistical analysis

Statistical analyses were performed using SPSS v 25.0 software (SPSS, Chicago, IL, USA).

Results

Labeling of cortical visuotactile connections with CTB

CTB injections sites in the visual cortex of intact mice (Fig. 1A) produced retrogradely labeled neuronal cell bodies in visual extrastriate cortices as well as in the barrel field of the somatosensory cortex (Fig. 1B). CTB injections in S1BF (Fig. 2A) labeled numerous neurons in the primary and secondary somatosensory, motor and visual cortices (Fig 2B).

CTB injections sites in the visual cortex of enucleated mice (Fig. 1C) also produced retrogradely labeled neurons in visual extrastriate cortices as well as in the barrel field of the somatosensory cortex (Fig. 1D) and injections in S1BF (Fig. 2C) labeled numerous neurons in the primary and secondary somatosensory, motor and visual cortices (Fig 2D), none of the injections damaged the underlying white matter.

All the observed retrogradely labeled neurons were plotted in S1, S1BF, V2M and V2L following CTB injections in V1 and in M1, M2, S2 and V1, following CTB injections in S1BF. Quantifications of labeled neurons were performed in V2M, V2L, M1, M2 and S2 in order to compare the projections between V1 and S1 as a ratio of the number of labeled neurons in these areas over the total number of labeled neurons rather than absolute numbers of neurons, which are directly related to the differences in injection size.

The number of labeled neurons varied between cases (Table 2), even though all injections were performed with the same parameters. A direct comparison of the absolute number of neurons can be considered but with certain reservations. In order to normalize for the differences in the total number of neurons that might arise through differences in injection size and tracer uptake efficacy, comparisons of the percentage of labeled neurons found in

each cortical area under study over the total number of neurons charted in them were done. Such comparisons are instructive of the relative weight of the projections and can show changes in the balance between projections. Quantifications for all cases are detailed for the intact and enucleated cases in table 2 and a comparison of the percentage of retrogradely labeled neurons in cortical areas is illustrated in figure 3A. Following injections of CTB in the primary visual cortex, the total number of retrogradely labeled neurons in the extrastriate cortical areas, V2M and V2L are comparable in the intact and enucleated mice but the number of labeled neurons found in the somatosensory cortices are reduced in the enucleated compared to the intact mice suggesting a relative reduction of the projections from the somatosensory cortices to the visual cortex (Table 2). Moreover, there were statistically significant differences in the percentage of labeled neurons observed in S1 and S1BF (Wilcoxon, $p = 0.032$) and V2M (Wilcoxon, $p = 0.016$) between the intact and enucleated cases following injections in V1 indicating a relative reduction of the inputs from the somatosensory cortices and V2M compared to the V2L projection to V1 (Fig. 3A).

Injections of CTB in the somatosensory cortices produce fewer retrogradely labeled neurons in all the studied areas in the enucleated mice than in the intact mice. Altered projections from the motor and secondary somatosensory areas were not expected in blind mice. This general reduction would more reasonably be explained by a systematic bias towards smaller injections in these cases (Table 2). In addition, there were no significant differences of the percentage of labeled neurons observed in M1, M2, S2 and V1 between the intact and the enucleated cases indicating that the relative weight of the projections was not modified by enucleation (Fig. 3A).

Significant differences in the percentage of labeled neurons in cortical layers were observed between the intact and enucleated cases following injections in V1 (Fig. 3B). A greater proportion of labeled neurons was found in layers 1 to 3 of S1 in the intact cases compared to the enucleated cases (Wilcoxon, $p = 0.032$). Significant differences in the percentage of labeled neurons in cortical layers were also observed between the intact and enucleated cases following injections in S1BF (Fig. 3C). A lesser proportion of labeled neurons was found in layer 5 of S2 in the intact cases compared to the enucleated cases (Wilcoxon, $p = 0.008$).

Laminar distribution of Cholera toxin b labeled neurons

Layer indices are summarized for the intact and enucleated cases in table 3 and illustrated in figure 4. Following CTB injections in V1 of the intact and the enucleated cases, there were more labeled neurons in infragranular than in supragranular layers of S1, S1BF, V2M and V2L. Hence, layer indices were negative in the majority of the cases, indicating the structure of a feedback projection to V1 from S1, S1BF, V2M and V2L. There was a statistically significant difference in the layer indices of S1 between intact and enucleated cases (Kruskal-Wallis, $p = 0.032$).

CTB injections in S1BF of the intact and the enucleated cases labeled more neurons in infragranular than in supragranular layers of M1, M2 and S2. Hence, layer indices were negative in the majority of the cases, suggestive of feedback projections to S1BF from M1, M2 and S2. There were labeled neurons in similar proportion in supra- and infragranular layers in V1 and, in all cases except one, layer indices were near zero, indicating a lateral type of connection between two primary sensory areas within the cortical network.

Laminar distribution of axonal swellings

An injection of BDA in V1 of intact and enucleated mice produced anterograde labeling of axons in S1, largely restricted to the barrelfield in each of the 10 cases. Labeled axons in S1BF were found in all cortical layers but were more numerous in infra- and supragranular layers, with a greater density especially in the supragranular layers 2/3. Labeling was similar in both the intact and enucleated cases, except that labeling in layer 1 had a greater density in the enucleated group compared to the intact group. Quite large swellings were observed in S1BF of intact (Fig. 5A) but not in the enucleated mice (Fig. 5B).

The laminar distribution of anterogradely labeled axons in V1 following an injection of BDA in S1BF of intact and enucleated mice was similar to that observed in S1BF following injections of BDA in V1. In both intact (Fig. 5C) and in enucleated mice (Fig. 5D) only quite small swellings were observed. None of the injections damaged the underlying white matter.

The injections of BDA in both V1 and S1BF of intact and enucleated mice resulted in anterograde axonal labeling in S1BF and V1 respectively, without signs of retrograde transport. In order to compare the labeling of axonal terminals in intact and enucleated cases, stereological estimates were performed of the laminar distribution of axonal swellings in S1BF and V1 (Figs. 6A and 6B respectively) following an injection of BDA in V1 and S1BF respectively.

There were no significant differences in the laminar distribution of axonal swellings in S1BF and V1 between the intact and enucleated cases. The stereologically estimated numbers of anterogradely labeled axonal swellings in each layer of S1 are given in table 4

and 5 for the intact and enucleated C57Bl/6 mice respectively and the numbers of anterogradely labeled axonal swellings in each layer of V1 are shown in table 6 and 7 for the intact and enucleated C57Bl/6 mice respectively.

Size distribution of axonal swellings in cortical layers

The size distribution of axonal swellings counted with the systematic stereological sampling was compared between the intact and enucleated groups for each cortical layer for the projection from V1 to S1BF (Fig. 7A-B) and from S1BF to V1 (Fig. 7C-D). The size of the axonal swellings ranged between 0.3 µm and 2 µm for the intact cases in the projection from V1 to S1BF and between 0.2 µm and 1.3 µm for the enucleated cases. The axonal swellings in S1BF of the intact group were larger than in the enucleated group in layers 1 to 3 (Kolmogorov-Smirnov tests, $p < 0.001$), layer 4 (Kolmogorov-Smirnov tests, $p < 0.001$), layer 5a (Kolmogorov-Smirnov tests, $p < 0.001$), layers 5b and 5c (Kolmogorov-Smirnov tests, $p < 0.001$) and layer 6 (Kolmogorov-Smirnov tests, $p = 0.001$) (Fig. 7B). The size of the axonal swellings ranged between 0.3 µm and 0.9 µm for the intact cases in the projection from S1BF to V1 and between 0.1 µm and 1.4 µm for the enucleated cases. The axonal swellings in V1 of the intact group were smaller than in the enucleated group in layers 1 to 3 (Kolmogorov-Smirnov tests, $p = 0.014$) and layer 4 (Kolmogorov-Smirnov tests, $p = 0.036$) (Fig. 7D).

Axonal thickness

The size distribution of the diameters of randomly sampled axons (Table 8) as they enter the grey matter was compared between the intact and enucleated cases for the projection from V1 to S1BF (Fig. 8A-C) and from S1BF to V1 (Fig. 8B-C). Axon thickness ranged

between 0.1 and 1.9 for the intact cases in the projection from V1 to S1BF and between 0.1 and 1.2 for the enucleated cases. The axons in S1BF of the intact group were larger than in the enucleated group (Kolmogorov-Smirnov tests, $p < 0.001$) (Fig. 8C). Axon thickness ranged between 0.1 and 0.5 for the intact cases in the projection from S1BF to V1 and between 0.1 and 0.7 for the enucleated cases. The axons in V1 of the intact group were not significantly different from the enucleated group (Fig. 8C).

Discussion

The effects of enucleation on V1 afferent projections

Visual input and spontaneous retinal activity play important roles in the determination of cortical areas and their connectivity (Pallas, 2001). Bilateral enucleation results in a significant reduction of the size of the lateral geniculate nucleus and/or V1 in the opossum (Karlen & Krubitzer, 2009), mouse (Heumann & Rabinowicz, 1980; Massé *et al.*, 2014), rat (Heumann & Rabinowicz, 1980), cat (Berman, 1991), and monkey (Rakic, 1988; Dehay *et al.*, 1989; Berman, 1991; Rakic *et al.*, 1991; Dehay *et al.*, 1996). Our results show that enucleation induces a slight reduction of the percentage of somatosensory projections to the visual cortex, but has no effect on the visual projections to the somatosensory cortex. This was previously demonstrated in the enucleated mice (Charbonneau *et al.*, 2012). We extend these findings with a comparison between the number of projecting neurons found inside the barrel field, the rest of S1 and inside the secondary somatosensory cortex, instead of considering the somatosensory cortex as a single area. Similarly, short transient reduction of somatosensory activity by the trimming of whiskers in the first five days after birth also significantly reduced the direct projection of the visual cortex to the somatosensory cortex cross-modal synchrony in S1 in adult rats (Sieben *et al.*, 2015). Conversely, bilateral enucleation on P10 in gerbil induced a slight relative increase of the number of labeled neurons in the primary somatosensory cortex compared to intact cases following a retrograde tracer injection in V1 in P28 animals (Henschke *et al.*, 2017). Species differences as well as timing of enucleations and sacrifices could explain this difference. A decreased functional connectivity between the visual cortex and the somatosensory cortex has been reported in blind humans (Yu *et al.*, 2008). This reduction

in connectivity following visual deprivation could be specific to the somatosensory modality, since the number of neurons projecting from the primary auditory cortex to V1 was not altered by early enucleation in mice (Charbonneau *et al.*, 2012) and gerbil (Henschke *et al.*, 2017). Moreover, there are no major changes in cross-modal connectivity patterns in deaf cats and ferrets (Meredith *et al.*, 2016). Conversely, a transient visual deprivation in early life in humans, results in auditory activation of the visual cortex, and this activation was interpreted as resulting from maintained exuberant cross-modal corticocortical projections that would otherwise be pruned out by normal visual activity during development (Collignon *et al.*, 2015).

Our results show that binocular enucleation at birth modifies the development of the feedback projections from extrastriate cortical areas in mice. Indeed, there was a reduced proportion of labeled neurons in V2M, whereas the proportion of labeled neurons was not changed in V2L in the enucleated mice. The mouse visual cortex comprises several extrastriate visual areas (Olavarria *et al.*, 1982; Olavarria & Montero, 1989; Wang & Burkhalter, 2007) that have distinct connectivity patterns (Wang *et al.*, 2011; Wang *et al.*, 2012) and functional properties (Andermann *et al.*, 2011; Marshel *et al.*, 2011; Glickfeld *et al.*, 2013; Matsui & Ohki, 2013; Glickfeld *et al.*, 2014). In the mouse, the medial/anterior extrastriate areas have similar connectivity patterns to dorsal stream areas in primates and lateral areas to ventral stream areas (Wang *et al.*, 2012). Our present results suggest that in mice, the development of feedback projections to V1 from the medial/dorsal stream areas might be more dependent on normal visual input.

The effects of enucleation on the somatosensory barrel field afferent projections

Our results also show that the projection to the somatosensory cortex from motor areas M1 and M2, S2 and the primary visual cortex V1 were not modified by early enucleation in mice. There are a few studies on the effects of sensory deprivation on the cortices dedicated to the spared sensory modalities. For example, in mice, dark rearing induces an increased size of the auditory cortex (Gyllensten *et al.*, 1965) whereas enucleation increases the size of the somatosensory cortex and barrel field (Bronchti *et al.*, 1992; Rauschecker *et al.*, 1992). There is also an increased density of dendritic spines in the auditory cortex following visual or tactile deprivation in rats (Ryugo *et al.*, 1975). Moreover, dark exposure in rats induces a reduction in the expression levels of GluR1 subunits and AMPA receptor mediated miniature EPSCs in the auditory and somatosensory cortices (Goel *et al.*, 2006; Jitsuki *et al.*, 2011) and potentiates thalamocortical inputs in the primary auditory cortex (Petrus *et al.*, 2014; Petrus *et al.*, 2015). There is only one other study on the connectivity of cortical areas of spared sensory modalities following sensory deprivations (Henschke *et al.*, 2017). Auditory, somatosensory and visual deprivations in gerbils increased connections between primary sensory cortices of the deprived and also of the spared senses (Henschke *et al.*, 2017). However, even though visual deprivation increased the afferent connections of the visual cortex, it had no effect on the afferent connections of the somatosensory cortex (Henschke *et al.*, 2017) as we show here in the mouse. Together, these studies indicate that the connectivity of the somatosensory cortex, although importantly modified by auditory and somatosensory deprivations, seem quite impervious to visual deprivation.

The effects of enucleation on the structure of the projections between V1 and S1

In addition to the relative reduction of the number of neurons of S1 projecting to V1 in the enucleated mice (Charbonneau *et al.*, 2012), we further show that this is mainly explained by a relative reduction of supragranular layer projection neurons of S1 and a shift towards more negative values of the layer index for this projection. Similarly, following auditory, somatosensory and visual deprivation in gerbils, layer indices of both the projections between V1 and S1 become more negative owing to a greater contribution of infragranular layer neurons to these projections (Henschke *et al.*, 2017). This contrasts with shift towards more positive values of layer indices of other connections between primary sensory cortices induced by auditory and somatosensory deprivation in gerbil indicating a greater contribution of supragranular projection neurons (Henschke *et al.*, 2017). Similarly, prenatal enucleation in monkey resulted in an increase proportion of supragranular layers projection neurons in the feedback projections from extrastriate cortices maintaining an immature laminar distribution of projections neurons and features of feedforward projections. This pathway specific laminar distribution of projection neurons emerges from an initial uniform laminar distribution of neurons mainly through selective elimination of supragranular layer projections in corticocortical feedback (Kennedy *et al.*, 1989; Batardiere *et al.*, 1998; Batardiere *et al.*, 2002) as well as in interhemispheric callosal projections (Innocenti & Frost, 1980). Several studies have shown that normal visual experience is necessary for the development of a normal complement of callosal projections and that altered visual experience results in the supranormal elimination of callosal projections of supragranular layer neurons (Innocenti & Frost, 1980; Innocenti *et al.*, 1985; Frost & Moy, 1989; Frost *et al.*, 1990; Boire *et al.*, 1995). Therefore, as in cats,

normal visual input is required for the normal establishment of supragranular layers projections in the cortex of the mouse. The differences of the effects of enucleation on the laminar distribution of supragranular projections neurons in monkeys, gerbils and mice might arise through differences in the timing of enucleations and age at which neuronal tracing experiments were performed and species differences. In the present study, enucleations were performed at birth and tracing experiments were carried out in adults. The gerbils were enucleated 10 days after birth and studied at 28 days of age and monkeys were enucleated prenatally and studied in infant (25 days old) and 10 months old.

The structure of feedforward and feedback corticocortical projections are defined by the laminar distribution of terminal labeling and neurons in the area the projection originates from. Indeed, in primates, feedforward projections are directed more specifically to granular layer 4 and feedback projections mostly target supragranular layers (Rockland & Pandya, 1979). These criteria were used to devise cortical hierarchies in primates (Felleman & Van Essen, 1991; Markov *et al.*, 2014). In rodents, feedforward projections target all cortical layers whereas feedback projections target both supra- and infragranular layers and generally avoid granular layer 4 (Coogan & Burkhalter, 1990; 1993). In rodents, the proposal for a hierarchical structure of visual cortical areas is based on the laminar distribution of terminal labeling only (Coogan & Burkhalter, 1993). The laminar distribution of retrogradely labeled neurons shows that the feedback type projection from the somatosensory cortex to the visual cortex is reciprocated by a lateral type projection in mouse and gerbil (Henschke *et al.*, 2015; Massé *et al.*, 2016). The reduction in the relative number of labeled neurons in the supragranular layers of the somatosensory cortex following CTB injections in V1 reduced the layer index value for this projection, making

it more strongly feedback. We would have expected that this would also modify the laminar distribution of axonal swellings anterogradely labeled in the somatosensory cortex after BDA injections in V1, namely through a reduction in the projection to layer 4. This was not the case. Indeed, there were no significant difference between the laminar distribution of axonal swellings in the visual and somatosensory cortices in intact and enucleated mice suggesting that these two features might be decoupled. This could be that a dichotomous classification of cortical projections in feedforward and feedback types might not apply to projections between primary sensory cortices.

The effects of enucleation on the thickness of axons and size axonal swellings

Visual deprivation also affected the size of axonal swellings in the projection from the visual cortex to the barrel field of the primary somatosensory cortex. Indeed, the larger axonal swellings observed in this projection in the intact mice were no longer present in the enucleated mice. There is evidence for two types of glutamatergic synaptic contacts in corticocortical connections (Covic & Sherman, 2011; De Pasquale & Sherman, 2011; Petrof & Sherman, 2013). Class 1B synapses are anatomically correlated with larger synaptic terminals and Class 2 with smaller synaptic terminals (Sherman & Guillery, 2013). Class 1B and 2 are respectively considered drivers and modulators (Sherman & Guillery, 1996; 1998; Reichova & Sherman, 2004; Lee & Sherman, 2008; 2009; Viaene *et al.*, 2011; Petrof & Sherman, 2013; Sherman & Guillery, 2013). We surmise that the larger swellings in the projection from V1 to S1BF in our results reflect a greater proportion of Class 1B terminals therein and that the large population of smaller swellings, which appears to be predominant in both projections, to be Class 2 terminals (Massé *et al.*, 2016). Axonal bouton size is positively correlated with the number of synaptic vesicles, active

zone area and the number of active zones (Streichert & Sargent, 1989; Yeow & Peterson, 1991; Pierce & Mendell, 1993; Pierce & Lewin, 1994; Harris & Sultan, 1995; Schikorski & Stevens, 1997; 1999). The reduced axonal swelling size in the projection from V1 to the barrel field in the enucleated mice suggests that afferent sensory activity is required for their normal development. Our results also show that the size distribution of the smaller terminals is shifted towards lower diameter values, suggesting that the size of all terminals is equally affected by the altered activity in the visual cortex of the enucleated mice. Similarly, intracortical synapses in layers 2/3 are depressed following dark exposure (Petrus *et al.*, 2015). In addition, a few large axonal swellings were found in layers 2/3 of the projection from S1BF to V1 in the enucleated mice. This could reflect cross-modal effects such as the potentiation of intracortical projections to layers 2/3 in dark exposed mice (Petrus *et al.*, 2015). Similarly, early deafness in cats increases dendritic spine density and size in supragranular layer neurons of the primary visual cortex (Clemo *et al.*, 2017). This could indicate, as in deaf cats, that supragranular layers of V1 could likely be activated by the already present cross-modal corticocortical afferents to the primary visual cortex in mice (Charbonneau *et al.*, 2012).

Different corticocortical projections include axons of different diameters depending on their source and the cortical areas they target (Anderson & Martin, 2002; Caminiti *et al.*, 2009; Tomasi *et al.*, 2012; Caminiti *et al.*, 2013; Innocenti *et al.*, 2014). The range of axonal diameters was greater in the visual cortex projections to the barrel field than in the reciprocal projection back to V1 and was significantly reduced in the enucleated mice. This reduction is commensurate with the axonal swelling size reduction in these mice. Indeed, the bouton size and axonal thickness are positively correlated in corticocortical projections

(Innocenti & Caminiti, 2017). Few studies have examined the effects of sensory activity on the diameter of axons in corticocortical connections. We know of no reports on the role of sensory afferent activity on the structure of single axons in corticocortical interareal projections activity. There are some indications that axonal structure would be altered by sensory deprivation. For example, the topography of striate extrastriate projections is abnormal in anophthalmic and in enucleated mice (Laramée *et al.*, 2014) and in enucleated rats (Cheetham *et al.*, 2007; Bruno *et al.*, 2009; Laing *et al.*, 2012; Laing *et al.*, 2013). The changes observed here in the size distribution of axonal swellings and diameter might reflect further changes in branching structure and terminal field size of axons.

Conclusions

In the current study, we asked how visual experience shapes cortical circuitry by comparing the direct reciprocal cross-modal corticocortical connections between V1 and S1 in intact and C57Bl/6 mice enucleated at birth, and determining quantitative differences and laminar distribution of neurons and terminals in these projections. We show that enucleation induced a relative reduction of the somatosensory projections to the visual cortex without affecting the visual, motor and somatosensory afferents to the somatosensory cortex. This reduction in connectivity is attributed to a greater reduction of the proportion of projecting neurons in the supragranular layers of S1, reinforcing the feedback structure of this projection. Enucleation also reduced the size of axonal swellings in all layers in the projection from the visual to the somatosensory cortex whereas some larger terminals appeared in the projection from the somatosensory cortex to the supragranular layers of the visual cortex. This shows pathway and laminar specific changes in cortical circuitry following loss of sensory afferent activity that could allow for cross-modal activation of the visual cortex in mice.

Acknowledgements

We are grateful to Nadia Desnoyers for animal care and maintenance. This work was supported by discovery grants of the Natural Sciences and Engineering Research Council of Canada (NSERC) to DB and GB, and a Canadian Foundation for Innovation Leader grant to DB.

Table legends

TABLE 1: Summary of the number of cases for each surgical condition that received B-fragment of cholera toxin (CTB) or biotinylated dextran amine (BDA) injections in the primary visual cortex (V1) or the barrel field of the primary somatosensory cortex (S1BF).

TABLE 2: Number and percentage (in parentheses) of retrogradely labeled neurons in neocortical areas after injections of CTB into the primary visual cortex (V1) and the primary somatosensory cortex (S1) of intact and enucleated C57Bl⁄6 mice.

TABLE 3: Numbers of retrogradely labeled neurons in layers 1-3/4/5/6 and layer indices (below) in neocortical areas after injections of CTB into the primary visual cortex (V1) and the primary somatosensory cortex (S1) of intact and enucleated C57Bl⁄6 mice.

TABLE 4: Stereological sampling parameters for the estimation of the number of anterogradely labeled axonal swellings in each layer in S1BF after injections of BDA into V1 of intact C57Bl/6 mice.

TABLE 5: Stereological sampling parameters for the estimation of the number of anterogradely labeled axonal swellings in each layer in S1BF after injections of BDA into V1 of enucleated C57Bl/6 mice.

TABLE 6: Stereological sampling parameters for the estimation of the number of anterogradely labeled axonal swellings in each layer in V1 after injections of BDA into S1BF of intact C57Bl/6 mice.

TABLE 7: Stereological sampling parameters for the estimation of the number of anterogradely labeled axonal swellings in each layer in V1 after injections of BDA into S1BF of enucleated C57Bl/6 mice.

TABLE 8: Sampling parameters for the estimation of the diameter of anterogradely labeled axons as they enter the grey matter in S1BF and V1 after injections of BDA into V1 and S1BF respectively of intact and enucleated at birth C57Bl/6 mice.

Figure legends

FIGURE 1: A: An injection of CTB in V1 of intact C57Bl/6 mice produced in B: Anterograde and retrograde labeling in S1BF. C: An injection of CTB in V1 of enucleated C57Bl/6 mice produced in D: Anterograde and retrograde labeling in S1BF. Scales: 1000 μm (A/C) and 200 μm (B/D).

FIGURE 2: A: An injection of CTB in S1BF of intact C57Bl/6 mice produced in B: Anterograde and retrograde labeling in V1. C: An injection of CTB in S1BF of enucleated C57Bl/6 mice produced in D: Anterograde and retrograde labeling in V1. Scales: 1000 μm (A/C) and 200 μm (B/D).

FIGURE 3: A: Percentage of retrogradely labeled neurons in cortical areas following an injection of CTB in V1 and S1BF. B and C: Percentage of retrogradely labeled neurons in each cortical layer following an injection of CTB in V1 (B) and in S1BF (C). Mean values are represented as a horizontal line in each individual graph.

FIGURE 4: Layer indices for neocortical areas following an injection of CTB in V1 and S1BF. Mean values are represented as a horizontal line in each individual graph.

FIGURE 5: High power photomicrographs of swellings in S1BF of intact and enucleated mice (A and B resp) following an injection of BDA in V1. High power photomicrographs of swellings in V1 of intact and enucleated mice (C and D resp) following an injection of BDA in S1BF. Small arrows point larger axonal swellings and large arrows point smaller swellings. Scales: 10 μm.

FIGURE 6: Laminar distribution of the number of axonal swellings in S1BF (A) and V1 (B) following an injection of BDA in V1 and S1BF respectively of intact and enucleated mice. n= number of counted swellings.

FIGURE 7: Size distribution (A and C) and box plot representation (B and D) of axonal swelling size in S1BF (A and B) and V1 (C and D) following injections of BDA in V1 and S1BF respectively of intact and enucleated mice. The box plots depict the minimum and maximum values, the upper (Q3) and lower (Q1) quartiles and the median.

FIGURE 8: Size distribution (A and B) and box plot representation (C) of the diameters of randomly sampled axons as they enter the grey matter in S1BF (A and C) and V1 (B and C) following an injection of BDA in V1 and S1BF respectively of intact and enucleated mice.

References:

Allman, B.L., Keniston, L.P. & Meredith, M.A. (2009) Adult deafness induces somatosensory conversion of ferret auditory cortex. *Proc Natl Acad Sci U S A*, **106**, 5925-5930.

Andermann, M.L., Kerlin, A.M., Roumis, D.K., Glickfeld, L.L. & Reid, R.C. (2011) Functional specialization of mouse higher visual cortical areas. *Neuron*, **72**, 1025-1039.

Anderson, J.C. & Martin, K.A. (2002) Connection from cortical area V2 to MT in macaque monkey. *J Comp Neurol*, **443**, 56-70.

Barone, P., Batardiere, A., Knoblauch, K. & Kennedy, H. (2000) Laminar distribution of neurons in extrastriate areas projecting to visual areas V1 and V4 correlates with the hierarchical rank and indicates the operation of a distance rule. *J Neurosci*, **20**, 3263-3281.

Barone, P., Lacassagne, L. & Kral, A. (2013) Reorganization of the connectivity of cortical field DZ in congenitally deaf cat. *PLoS One*, **8**, e60093.

Batardiere, A., Barone, P., Dehay, C. & Kennedy, H. (1998) Area-specific laminar distribution of cortical feedback neurons projecting to cat area 17: quantitative analysis in the adult and during ontogeny. *J Comp Neurol*, **396**, 493-510.

Batardiere, A., Barone, P., Knoblauch, K., Giroud, P., Berland, M., Dumas, A.M. & Kennedy, H. (2002) Early specification of the hierarchical organization of visual cortical areas in the macaque monkey. *Cereb Cortex*, **12**, 453-465.

Berezovskii, V.K., Nassi, J.J. & Born, R.T. (2011) Segregation of feedforward and feedback projections in mouse visual cortex. *J Comp Neurol*, **519**, 3672-3683.

Berman, N.E. (1991) Alterations of visual cortical connections in cats following early removal of retinal input. *Brain Res Dev Brain Res*, **63**, 163-180.

Bizley, J.K., Nodal, F.R., Bajo, V.M., Nelken, I. & King, A.J. (2007) Physiological and anatomical evidence for multisensory interactions in auditory cortex. *Cereb Cortex*, **17**, 2172-2189.

Boire, D., Morris, R., Ptito, M., Lepore, F. & Frost, D.O. (1995) Effects of neonatal splitting of the optic chiasm on the development of feline visual callosal connections. *Exp Brain Res*, **104**, 275-286.

Bronchti, G., Schonenberger, N., Welker, E. & Van der Loos, H. (1992) Barrelfield expansion after neonatal eye removal in mice. *Neuroreport*, **3**, 489-492.

Bruno, R.M., Hahn, T.T., Wallace, D.J., de Kock, C.P. & Sakmann, B. (2009) Sensory experience alters specific branches of individual corticocortical axons during development. *J Neurosci*, **29**, 3172-3181.

Budinger, E., Heil, P., Hess, A. & Scheich, H. (2006) Multisensory processing via early cortical stages: Connections of the primary auditory cortical field with other sensory systems. *Neuroscience*, **143**, 1065-1083.

Budinger, E., Laszcz, A., Lison, H., Scheich, H. & Ohl, F.W. (2008) Non-sensory cortical and subcortical connections of the primary auditory cortex in Mongolian gerbils: bottom-up and top-down processing of neuronal information via field AI. *Brain Res*, **1220**, 2-32.

Budinger, E. & Scheich, H. (2009) Anatomical connections suitable for the direct processing of neuronal information of different modalities via the rodent primary auditory cortex. *Hear Res*, **258**, 16-27.

Butler, B.E., Chabot, N. & Lomber, S.G. (2016a) Quantifying and comparing the pattern of thalamic and cortical projections to the posterior auditory field in hearing and deaf cats. *J Comp Neurol*, **524**, 3042-3063.

Butler, B.E., Chabot, N. & Lomber, S.G. (2016b) A quantitative comparison of the hemispheric, areal, and laminar origins of sensory and motor cortical projections to the superior colliculus of the cat. *J Comp Neurol*, **524**, 2623-2642.

Caminiti, R., Carducci, F., Piervincenzi, C., Battaglia-Mayer, A., Confalone, G., Visco-Comandini, F., Pantano, P. & Innocenti, G.M. (2013) Diameter, length, speed, and conduction delay of callosal axons in macaque monkeys and humans: comparing data from histology and magnetic resonance imaging diffusion tractography. *J Neurosci*, **33**, 14501-14511.

Caminiti, R., Ghaziri, H., Galuske, R., Hof, P.R. & Innocenti, G.M. (2009) Evolution amplified processing with temporally dispersed slow neuronal connectivity in primates. *Proc Natl Acad Sci U S A*, **106**, 19551-19556.

Campi, K.L., Bales, K.L., Grunewald, R. & Krubitzer, L. (2010) Connections of auditory and visual cortex in the prairie vole (Microtus ochrogaster): evidence for multisensory processing in primary sensory areas. *Cereb Cortex*, **20**, 89-108.

Cappe, C. & Barone, P. (2005) Heteromodal connections supporting multisensory integration at low levels of cortical processing in the monkey. *Eur J Neurosci*, **22**, 2886-2902.

Caviness, V.S., Jr. (1975) Architectonic map of neocortex of the normal mouse. *J Comp Neurol*, **164**, 247-263.

Chabot, N., Butler, B.E. & Lomber, S.G. (2015) Differential Modification of Cortical and Thalamic Projections to Cat Primary Auditory Cortex Following Early- and Late-Onset Deafness. *J Comp Neurol*, **523**, 2297-2320.

Charbonneau, V., Laramee, M.E., Boucher, V., Bronchti, G. & Boire, D. (2012) Cortical and subcortical projections to primary visual cortex in anophthalmic, enucleated and sighted mice. *Eur J Neurosci*, **36**, 2949-2963.

Cheetham, C.E., Hammond, M.S., Edwards, C.E. & Finnerty, G.T. (2007) Sensory experience alters cortical connectivity and synaptic function site specifically. *J Neurosci*, **27**, 3456-3465.

Clavagnier, S., Falchier, A. & Kennedy, H. (2004) Long-distance feedback projections to area V1: implications for multisensory integration, spatial awareness, and visual consciousness. *Cogn Affect Behav Neurosci*, **4**, 117-126.

Clemo, H.R., Lomber, S.G. & Meredith, M.A. (2017) Synaptic distribution and plasticity in primary auditory cortex (A1) exhibits laminar and cell-specific changes in the deaf. *Hear Res*, **353**, 122-134.

Collignon, O., Dormal, G., de Heering, A., Lepore, F., Lewis, T.L. & Maurer, D. (2015) Long-Lasting Crossmodal Cortical Reorganization Triggered by Brief Postnatal Visual Deprivation. *Curr Biol*, **25**, 2379-2383.

Coogan, T.A. & Burkhalter, A. (1988) Sequential development of connections between striate and extrastriate visual cortical areas in the rat. *J Comp Neurol*, **278**, 242-252.

Coogan, T.A. & Burkhalter, A. (1990) Conserved patterns of cortico-cortical connections define areal hierarchy in rat visual cortex. *Exp Brain Res*, **80**, 49-53.

Coogan, T.A. & Burkhalter, A. (1993) Hierarchical organization of areas in rat visual cortex. *J Neurosci*, **13**, 3749-3772.

Covic, E.N. & Sherman, S.M. (2011) Synaptic properties of connections between the primary and secondary auditory cortices in mice. *Cereb Cortex*, **21**, 2425-2441.

De Pasquale, R. & Sherman, S.M. (2011) Synaptic properties of corticocortical connections between the primary and secondary visual cortical areas in the mouse. *J Neurosci*, **31**, 16494-16506.

Dehay, C., Giroud, P., Berland, M., Killackey, H. & Kennedy, H. (1996) Contribution of thalamic input to the specification of cytoarchitectonic cortical fields in the primate: effects of bilateral enucleation in the fetal monkey on the boundaries, dimensions, and gyrification of striate and extrastriate cortex. *J Comp Neurol*, **367**, 70-89.

Dehay, C., Horsburgh, G., Berland, M., Killackey, H. & Kennedy, H. (1989) Maturation and connectivity of the visual cortex in monkey is altered by prenatal removal of retinal input. *Nature*, **337**, 265-267.

Falchier, A., Clavagnier, S., Barone, P. & Kennedy, H. (2002) Anatomical evidence of multimodal integration in primate striate cortex. *J Neurosci*, **22**, 5749-5759.

Felleman, D.J. & Van Essen, D.C. (1991) Distributed hierarchical processing in the primate cerebral cortex. *Cereb Cortex*, **1**, 1-47.

Foxe, J.J., Morocz, I.A., Murray, M.M., Higgins, B.A., Javitt, D.C. & Schroeder, C.E. (2000) Multisensory auditory-somatosensory interactions in early cortical

processing revealed by high-density electrical mapping. *Brain Res Cogn Brain Res*, **10**, 77-83.

Franklin, B.J. & Paxinos, G. (2008) *The Mouse Brain in Stereotaxic Coordinates*. Academic Press, San Diego.

Frost, D.O. & Moy, Y.P. (1989) Effects of dark rearing on the development of visual callosal connections. *Exp Brain Res*, **78**, 203-213.

Frost, D.O., Moy, Y.P. & Smith, D.C. (1990) Effects of alternating monocular occlusion on the development of visual callosal connections. *Exp Brain Res*, **83**, 200-209.

Ghazanfar, A.A. & Schroeder, C.E. (2006) Is neocortex essentially multisensory? *Trends Cogn Sci*, **10**, 278-285.

Glickfeld, L.L., Andermann, M.L., Bonin, V. & Reid, R.C. (2013) Cortico-cortical projections in mouse visual cortex are functionally target specific. *Nat Neurosci*, **16**, 219-226.

Glickfeld, L.L., Reid, R.C. & Andermann, M.L. (2014) A mouse model of higher visual cortical function. *Curr Opin Neurobiol*, **24**, 28-33.

Goel, A., Jiang, B., Xu, L.W., Song, L., Kirkwood, A. & Lee, H.K. (2006) Cross-modal regulation of synaptic AMPA receptors in primary sensory cortices by visual experience. *Nat Neurosci*, **9**, 1001-1003.

Gyllensten, L., Malmofors, T. & Norrlin , M.L. (1965) Effect of visusal deprivation on the optic centers of the growing and adult mice. *J Comp Neurol*, **124**, 149-160.

Hackett, T.A., De La Mothe, L.A., Ulbert, I., Karmos, G., Smiley, J. & Schroeder, C.E. (2007) Multisensory convergence in auditory cortex, II. Thalamocortical connections of the caudal superior temporal plane. *J Comp Neurol*, **502**, 924-952.

Harris, K.M. & Sultan, P. (1995) Variation in the number, location and size of synaptic vesicles provides an anatomical basis for the nonuniform probability of release at hippocampal CA1 synapses. *Neuropharmacology*, **34**, 1387-1395.

Henschke, J.U., Noesselt, T., Scheich, H. & Budinger, E. (2015) Possible anatomical pathways for short-latency multisensory integration processes in primary sensory cortices. *Brain Struct Funct*, **220**, 955-977.

Henschke, J.U., Oelschlegel, A.M., Angenstein, F., Ohl, F.W., Goldschmidt, J., Kanold, P.O. & Budinger, E. (2017) Early sensory experience influences the development of multisensory thalamocortical and intracortical connections of primary sensory cortices. *Brain Struct Funct*.

Heumann, D. & Rabinowicz, T. (1980) Postnatal development of the dorsal lateral geniculate nucleus in the normal and enucleated albino mouse. *Exp Brain Res*, **38**, 75-85.

Hilgetag, C.C. & Grant, S. (2000) Uniformity, specificity and variability of corticocortical connectivity. *Philos Trans R Soc Lond B Biol Sci*, **355**, 7-20.

Hilgetag, C.C., O'Neill, M.A. & Young, M.P. (2000) Hierarchical organization of macaque and cat cortical sensory systems explored with a novel network processor. *Philos Trans R Soc Lond B Biol Sci*, **355**, 71-89.

Innocenti, G.M. & Caminiti, R. (2017) Axon diameter relates to synaptic bouton size: structural properties define computationally different types of cortical connections in primates. *Brain Struct Funct*, **222**, 1169-1177.

Innocenti, G.M. & Frost, D.O. (1980) The postnatal development of visual callosal connections in the absence of visual experience or of the eyes. *Exp Brain Res*, **39**, 365-375.

Innocenti, G.M., Frost, D.O. & Illes, J. (1985) Maturation of visual callosal connections in visually deprived kittens: a challenging critical period. *J Neurosci*, **5**, 255-267.

Innocenti, G.M. & Price, D.J. (2005) Exuberance in the development of cortical networks. *Nat Rev Neurosci*, **6**, 955-965.

Innocenti, G.M., Vercelli, A. & Caminiti, R. (2014) The diameter of cortical axons depends both on the area of origin and target. *Cereb Cortex*, **24**, 2178-2188.

Iurilli, G., Ghezzi, D., Olcese, U., Lassi, G., Nazzaro, C., Tonini, R., Tucci, V., Benfenati, F. & Medini, P. (2012) Sound-driven synaptic inhibition in primary visual cortex. *Neuron*, **73**, 814-828.

Jitsuki, S., Takemoto, K., Kawasaki, T., Tada, H., Takahashi, A., Becamel, C., Sano, A., Yuzaki, M., Zukin, R.S., Ziff, E.B., Kessels, H.W. & Takahashi, T. (2011) Serotonin mediates cross-modal reorganization of cortical circuits. *Neuron*, **69**, 780-792.

Karlen, S.J., Kahn, D.M. & Krubitzer, L. (2006) Early blindness results in abnormal corticocortical and thalamocortical connections. *Neuroscience*, **142**, 843-858.

Karlen, S.J. & Krubitzer, L. (2009) Effects of bilateral enucleation on the size of visual and nonvisual areas of the brain. *Cereb Cortex*, **19**, 1360-1371.

Kayser, C. (2010) The multisensory nature of unisensory cortices: a puzzle continued. *Neuron*, **67**, 178-180.

Kayser, C. & Logothetis, N.K. (2007) Do early sensory cortices integrate cross-modal information? *Brain Struct Funct*, **212**, 121-132.

Kennedy, H., Bullier, J. & Dehay, C. (1989) Transient projection from the superior temporal sulcus to area 17 in the newborn macaque monkey. *Proc Natl Acad Sci U S A*, **86**, 8093-8097.

Khalil, R. & Levitt, J.B. (2014) Developmental remodeling of corticocortical feedback circuits in ferret visual cortex. *J Comp Neurol*, **522**, 3208-3228.

Kok, M.A., Chabot, N. & Lomber, S.G. (2014) Cross-modal reorganization of cortical afferents to dorsal auditory cortex following early- and late-onset deafness. *J Comp Neurol*, **522**, 654-675.

Laing, R.J., Bock, A.S., Lasiene, J. & Olavarria, J.F. (2012) Role of retinal input on the development of striate-extrastriate patterns of connections in the rat. *J Comp Neurol*, **520**, 3256-3276.

Laing, R.J., Lasiene, J. & Olavarria, J.F. (2013) Topography of striate-extrastriate connections in neonatally enucleated rats. *Biomed Res Int*, **2013**, 592426.

Lakatos, P., Chen, C.M., O'Connell, M.N., Mills, A. & Schroeder, C.E. (2007) Neuronal oscillations and multisensory interaction in primary auditory cortex. *Neuron*, **53**, 279-292.

Laramée, M.E., Bronchti, G. & Boire, D. (2014) Primary visual cortex projections to extrastriate cortices in enucleated and anophthalmic mice. *Brain Struct Funct*, **219**, 2051-2070.

Laramee, M.E., Kurotani, T., Rockland, K.S., Bronchti, G. & Boire, D. (2011) Indirect pathway between the primary auditory and visual cortices through layer V pyramidal neurons in V2L in mouse and the effects of bilateral enucleation. *Eur J Neurosci*, **34**, 65-78.

Larsen, D.D., Luu, J.D., Burns, M.E. & Krubitzer, L. (2009) What are the Effects of Severe Visual Impairment on the Cortical Organization and Connectivity of Primary Visual Cortex? *Front Neuroanat*, **3**, 30.

Lee, C.C. & Sherman, S.M. (2008) Synaptic properties of thalamic and intracortical inputs to layer 4 of the first- and higher-order cortical areas in the auditory and somatosensory systems. *J Neurophysiol*, **100**, 317-326.

Lee, C.C. & Sherman, S.M. (2009) Modulator property of the intrinsic cortical projection from layer 6 to layer 4. *Front Syst Neurosci*, **3**, 3.

Lewis, R. & Noppeney, U. (2010) Audiovisual synchrony improves motion discrimination via enhanced connectivity between early visual and auditory areas. *J Neurosci*, **30**, 12329-12339.

Liang, M., Mouraux, A., Hu, L. & Iannetti, G.D. (2013) Primary sensory cortices contain distinguishable spatial patterns of activity for each sense. *Nat Commun*, **4**, 1979.

Magrou, L., Barone, P., Markov, N.T., Killackey, H., Goiroud, P., Berland, M., Knoblauch, K., Dehay, C. & Kennedy, H. (2017) Cortical Connectivity In A Macaque Model Of Congenital Blindness *bioRxiv*.

Markov, N.T., Vezoli, J., Chameau, P., Falchier, A., Quilodran, R., Huissoud, C., Lamy, C., Misery, P., Giroud, P., Ullman, S., Barone, P., Dehay, C., Knoblauch, K. & Kennedy, H. (2014) Anatomy of hierarchy: feedforward and feedback pathways in macaque visual cortex. *J Comp Neurol*, **522**, 225-259.

Marshel, J.H., Garrett, M.E., Nauhaus, I. & Callaway, E.M. (2011) Functional specialization of seven mouse visual cortical areas. *Neuron*, **72**, 1040-1054.

Massé, I.O., Guillemette, S., Laramée, M.E., Bronchti, G. & Boire, D. (2014) Strain differences of the effect of enucleation and anophthalmia on the size and growth of sensory cortices in mice. *Brain Res*, **1588**, 113-126.

Massé, I.O., Ross, S., Bronchti, G. & Boire, D. (2016) Asymmetric Direct Reciprocal Connections Between Primary Visual and Somatosensory Cortices of the Mouse. *Cereb Cortex*.

Matsui, T. & Ohki, K. (2013) Target dependence of orientation and direction selectivity of corticocortical projection neurons in the mouse V1. *Front Neural Circuits*, **7**, 143.

Meredith, M.A. & Allman, B.L. (2012) Early hearing-impairment results in crossmodal reorganization of ferret core auditory cortex. *Neural Plast*, **2012**, 601591.

Meredith, M.A., Clemo, H.R., Corley, S.B., Chabot, N. & Lomber, S.G. (2016) Cortical and thalamic connectivity of the auditory anterior ectosylvian cortex of early-deaf cats: Implications for neural mechanisms of crossmodal plasticity. *Hear Res*, **333**, 25-36.

Meredith, M.A. & Lomber, S.G. (2017) Species-dependent role of crossmodal connectivity among the primary sensory cortices. *Hear Res*, **343**, 83-91.

Noesselt, T., Rieger, J.W., Schoenfeld, M.A., Kanowski, M., Hinrichs, H., Heinze, H.J. & Driver, J. (2007) Audiovisual temporal correspondence modulates human multisensory superior temporal sulcus plus primary sensory cortices. *J Neurosci*, **27**, 11431-11441.

Olavarria, J., Mignano, L.R. & Van Sluyters, R.C. (1982) Pattern of extrastriate visual areas connecting reciprocally with striate cortex in the mouse. *Exp Neurol*, **78**, 775-779.

Olavarria, J. & Montero, V.M. (1989) Organization of visual cortex in the mouse revealed by correlating callosal and striate-extrastriate connections. *Vis Neurosci*, **3**, 59-69.

Pallas, S.L. (2001) Intrinsic and extrinsic factors that shape neocortical specification. *Trends Neurosci*, **24**, 417-423.

Paperna, T. & Malach, R. (1991) Patterns of sensory intermodality relationships in the cerebral cortex of the rat. *J Comp Neurol*, **308**, 432-456.

Petrof, I. & Sherman, S.M. (2013) Functional significance of synaptic terminal size in glutamatergic sensory pathways in thalamus and cortex. *J Physiol*, **591**, 3125-3131.

Petrus, E., Isaiah, A., Jones, A.P., Li, D., Wang, H., Lee, H.K. & Kanold, P.O. (2014) Crossmodal induction of thalamocortical potentiation leads to enhanced information processing in the auditory cortex. *Neuron*, **81**, 664-673.

Petrus, E., Rodriguez, G., Patterson, R., Connor, B., Kanold, P.O. & Lee, H.K. (2015) Vision loss shifts the balance of feedforward and intracortical circuits in opposite directions in mouse primary auditory and visual cortices. *J Neurosci*, **35**, 8790-8801.

Pierce, J.P. & Lewin, G.R. (1994) An ultrastructural size principle. *Neuroscience*, **58**, 441-446.

Pierce, J.P. & Mendell, L.M. (1993) Quantitative ultrastructure of Ia boutons in the ventral horn: scaling and positional relationships. *J Neurosci*, **13**, 4748-4763.

Price, D.J., Kennedy, H., Dehay, C., Zhou, L., Mercier, M., Jossin, Y., Goffinet, A.M., Tissir, F., Blakey, D. & Molnar, Z. (2006) The development of cortical connections. *Eur J Neurosci*, **23**, 910-920.

Rakic, P. (1988) Specification of cerebral cortical areas. *Science*, **241**, 170-176.

Rakic, P., Suner, I. & Williams, R.W. (1991) A novel cytoarchitectonic area induced experimentally within the primate visual cortex. *Proc Natl Acad Sci U S A*, **88**, 2083-2087.

Rauschecker, J.P., Tian, B., Korte, M. & Egert, U. (1992) Crossmodal changes in the somatosensory vibrissa/barrel system of visually deprived animals. *Proc Natl Acad Sci U S A*, **89**, 5063-5067.

Reichova, I. & Sherman, S.M. (2004) Somatosensory corticothalamic projections: distinguishing drivers from modulators. *J Neurophysiol*, **92**, 2185-2197.

Rockland, K.S. & Pandya, D.N. (1979) Laminar origins and terminations of cortical connections of the occipital lobe in the rhesus monkey. *Brain Res*, **179**, 3-20.

Rohe, T. & Noppeney, U. (2016) Distinct Computational Principles Govern Multisensory Integration in Primary Sensory and Association Cortices. *Curr Biol*, **26**, 509-514.

Ryugo, D.K., Ryugo, R., Globus, A. & Killackey, H.P. (1975) Increased spine density in auditory cortex following visual or somatic deafferentation. *Brain Res*, **90**, 143-146.

Schikorski, T. & Stevens, C.F. (1997) Quantitative ultrastructural analysis of hippocampal excitatory synapses. *J Neurosci*, **17**, 5858-5867.

Schikorski, T. & Stevens, C.F. (1999) Quantitative fine-structural analysis of olfactory cortical synapses. *Proc Natl Acad Sci U S A*, **96**, 4107-4112.

Schroeder, C.E. & Foxe, J. (2005) Multisensory contributions to low-level, 'unisensory' processing. *Curr Opin Neurobiol*, **15**, 454-458.

Sherman, S.M. & Guillery, R.W. (1996) Functional organization of thalamocortical relays. *J Neurophysiol*, **76**, 1367-1395.

Sherman, S.M. & Guillery, R.W. (1998) On the actions that one nerve cell can have on another: distinguishing "drivers" from "modulators". *Proc Natl Acad Sci U S A*, **95**, 7121-7126.

Sherman, S.M. & Guillery, R.W. (2013) *Functional connections of cortical areas*. MIT Press, Cambridge MA, London England.

Sieben, K., Bieler, M., Roder, B. & Hanganu-Opatz, I.L. (2015) Neonatal Restriction of Tactile Inputs Leads to Long-Lasting Impairments of Cross-Modal Processing. *PLoS Biol*, **13**, e1002304.

Sieben, K., Roder, B. & Hanganu-Opatz, I.L. (2013) Oscillatory entrainment of primary somatosensory cortex encodes visual control of tactile processing. *J Neurosci*, **33**, 5736-5749.

Streichert, L.C. & Sargent, P.B. (1989) Bouton ultrastructure and synaptic growth in a frog autonomic ganglion. *J Comp Neurol*, **281**, 159-168.

Tomasi, S., Caminiti, R. & Innocenti, G.M. (2012) Areal differences in diameter and length of corticofugal projections. *Cereb Cortex*, **22**, 1463-1472.

Viaene, A.N., Petrof, I. & Sherman, S.M. (2011) Synaptic properties of thalamic input to layers 2/3 and 4 of primary somatosensory and auditory cortices. *J Neurophysiol*, **105**, 279-292.

Wang, Q. & Burkhalter, A. (2007) Area map of mouse visual cortex. *J Comp Neurol*, **502**, 339-357.

Wang, Q., Gao, E. & Burkhalter, A. (2011) Gateways of ventral and dorsal streams in mouse visual cortex. *J Neurosci*, **31**, 1905-1918.

Wang, Q., Sporns, O. & Burkhalter, A. (2012) Network analysis of corticocortical connections reveals ventral and dorsal processing streams in mouse visual cortex. *J Neurosci*, **32**, 4386-4399.

Wang, Y., Celebrini, S., Trotter, Y. & Barone, P. (2008) Visuo-auditory interactions in the primary visual cortex of the behaving monkey: electrophysiological evidence. *BMC Neurosci*, **9**, 79.

West, M.J. & Gundersen, H.J. (1990) Unbiased stereological estimation of the number of neurons in the human hippocampus. *J Comp Neurol*, **296**, 1-22.

West, M.J., Slomianka, L. & Gundersen, H.J. (1991) Unbiased stereological estimation of the total number of neurons in thesubdivisions of the rat hippocampus using the optical fractionator. *Anat Rec*, **231**, 482-497.

Yeow, M.B. & Peterson, E.H. (1991) Active zone organization and vesicle content scale with bouton size at a vertebrate central synapse. *J Comp Neurol*, **307**, 475-486.

Yu, C., Liu, Y., Li, J., Zhou, Y., Wang, K., Tian, L., Qin, W., Jiang, T. & Li, K. (2008) Altered functional connectivity of primary visual cortex in early blindness. *Hum Brain Mapp*, **29**, 533-543.

Zingg, B., Hintiryan, H., Gou, L., Song, M.Y., Bay, M., Bienkowski, M.S., Foster, N.N., Yamashita, S., Bowman, I., Toga, A.W. & Dong, H.W. (2014) Neural networks of the mouse neocortex. *Cell*, **156**, 1096-1111.

TABLE 1: Summary of the number of cases for each surgical condition that received B-fragment of cholera toxin (CTB) or biotinylated dextran amine (BDA) injections in the primary visual cortex (V1) or the barrel field of the primary somatosensory cortex (S1BF).

Tracer	Injection site	Surgical condition	Number of cases
CTB -retrograde-	V1	Intact	5
CTB -retrograde-	V1	Enucleated	5
CTB -retrograde-	S1BF	Intact	5
CTB -retrograde-	S1BF	Enucleated	5
BDA -anterograde-	V1	Intact	5
BDA -anterograde-	V1	Enucleated	5
BDA -anterograde-	S1BF	Intact	5
BDA -anterograde-	S1BF	Enucleated	5

TABLE 2: Number and percentage (in parentheses) of retrogradely labeled neurons in neocortical areas after injections of CTb into the primary visual cortex (V1) and the primary somatosensory cortex (S1) of intact and enucleated C57Bl/6 mice.

Injection site	Case	Cortical area			
		S1	S1BF	V2M	V2L
V1 Intact	CT9	85 (4.43)	164 (8.55)	448 (23.35)	1222 (63.68)
	CT20	16 (1.59)	10 (1.00)	183 (18.23)	795 (79.18)
	CT25	15 (1.87)	56 (6.97)	93 (11.58)	639 (79.58)
	CT26	39 (10.74)	112 (30.85)	45 (12.40)	167 (46.01)
	CT31	28 (3.14)	62 (6.94)	181 (20.67)	622 (69.65)
	Mean ± SEM	36.60 ± 14.39	80.80 ± 29.45	190.00 ± 77.91	689.00 ± 189.54
		(4.35 ± 1.87)	(10.86 ± 5.77)	(17.16 ± 2.54)	(67.62 ± 6.91)
V1 Enu	CT52	5 (0.52)	9 (0.94)	272 (28.42)	671 (70.12)
	CT53	5 (0.79)	2 (0.32)	143 (22.59)	483 (76.30)
	CT54	21 (1.14)	18 (0.98)	507 (27.63)	1289 (70.25)
	CT55	6 (0.76)	14 (1.77)	227 (28.63)	546 (68.85)
	CT57	28 (2.60)	12 (1.11)	333 (30.92)	704 (65.37)
	Mean ± SEM	13.00 ± 5.40	11.00 ± 3.00	296.40 ± 68.30	738.60 ± 160.30
		(1.16 ± 0.42)	(1.02 ± 0.26)	(27.64 ± 1.54)	(70.18 ± 1.98)

Injection site	Case	Cortical area			
		M1	M2	S2	V1
S1 Intact	03-02b7	148 (11.23)	209 (15.86)	415 (31.49)	546 (41.43)
	04-01b2	726 (37.10)	573 (29.28)	582 (29.74)	76 (3.88)
	03-02b4	800 (24.17)	1510 (45.62)	600 (18.13)	400 (12.09)
	03-02b5	929 (26.84)	1197 (34.59)	1181 (34.12)	154 (4.45)
	03-02b6	450 (23.40)	323 (16.80)	1117 (58.09)	33 (1.72)
	Mean ± SEM	610.60 ± 156.20	762.40 ± 283.17	779.00 ± 173.06	241.80 ± 110.78
		(24.55 ± 4.62)	(28.43 ± 6.26)	(34.31 ± 7.32)	(12.71 ± 8.26)
S1 Enu	1	313 (25.93)	574 (47.56)	243 (20.13)	77 (6.38)
	2	124 (11.05)	339 (30.21)	381 (33.96)	278 (24.78)
	3	328 (26.95)	617 (50.70)	220 (18.08)	52 (4.27)
	4	158 (11.41)	600 (43.32)	387 (27.94)	240 (17.33)
	5	115 (9.02)	535 (41.96)	409 (32.08)	216 (16.94)
	Mean ± SEM	207.60 ± 52.22	533.00 ± 56.38	328.00 ± 44.54	172.60 ± 50.76
		(16.87 ± 4.40)	(42.75 ± 3.91)	(26.44 ± 3.54)	(13.94 ± 4.25)

TABLE 3: Numbers of retrogradely labeled neurons in layers I-III/IV/V/VI and layer indices (below) in neocortical areas after injections of CTb into the primary visual cortex (V1) and the primary somatosensory cortex (S1) of intact and enucleated C57Bl⁄6 mice.

Injection site	Case	Cortical area			
		S1	S1BF	V2M	V2L
V1	CT9	14 / 11 / 33 / 27 -0.62	23 / 25 / 55 / 61 -0.67	106 / 50 / 219 / 73 -0.47	338 / 113 / 555 / 216 -0.39
Intact	CT20	4 / 0 / 9 / 3 -0.5	0 / 0 / 3 / 7 -1.00	42 / 14 / 111 / 16 -0.50	239 / 90 / 339 / 127 -0.32
	CT25	4 / 0 / 5 / 6 -0.47	13 / 0 / 27 / 16 -0.54	35 / 8 / 41 / 9 -0.18	333 / 67 / 195 / 44 0.16
	CT26	6 / 8 / 13 / 12 -0.61	19 / 6 / 41 / 46 -0.64	13 / 3 / 26 / 3 -0.38	57 / 5 / 70 / 35 -0.30
	CT31	11 / 1 / 8 / 8 -0.19	8 / 0 / 27 / 27 -0.74	67 / 14 / 86 / 14 -0.20	218 / 32 / 278 / 94 -0.26
	Mean Sup/Inf ± SEM	8 ± 2/25 ± 10 -0.52 ± 0.09	13 ± 5/62 ± 21 -0.66 ± 0.09	53 ± 18/120 ± 52 -0.39 ± 0.08	237 ± 57/391 ± 127 -0.25 ± 0.11
V1	CT52	1 / 0 / 1 / 3 -0.60	1 / 0 / 4 / 4 -0.78	83 / 66 / 110 / 13 -0.19	223 / 156 / 193 / 99 -0.13
Enu	CT53	0 / 1 / 4 / 0 -1.00	0 / 0 / 1 / 1 -1.00	41 / 31 / 57 / 14 -0.27	200 / 67 / 158 / 58 -0.04
	CT54	3 / 0 / 11 / 7 -0.71	2 / 4 / 3 / 9 -0.71	165 / 57 / 271 / 14 -0.27	461 / 191 / 495 / 142 -0.16
	CT55	0 / 1 / 3 / 2 -1.00	0 / 5 / 4 / 5 -1.00	67 / 2 / 145 / 13 -0.40	195 / 58 / 219 / 74 -0.20
	CT57	1 / 1 / 12 / 14 -0.93	0 / 1 / 9 / 2 -1.00	93 / 32 / 196 / 12 -0.38	238 / 80 / 296 /90 -0.24
	Mean Sup/Inf ± SEM	1 ± 1/11 ± 5 -0.84 ± 0.09	1 ± 0/8 ± 3 -0.87 ± 0.07	90 ± 23/169 ± 41 -0.31 ± 0.04	263 ± 56/365 ± 83 -0.16 ± 0.04

Injection site	Case	Cortical area			
		M1	M2	S2	V1
S1	03-02b7	81 / 0 / 58 / 9 0.10	103 / 0 / 104 / 2 -0.01	38 / 26 / 87 / 264 -0.81	216 / 94 / 137 / 99 -0.04
Intact	04-01b2	332 / 0 / 348 / 46 -0.09	340 / 0 / 221 / 12 0.19	122 / 47 / 142 / 271 -0.54	34 / 3 / 16 / 23 -0.07
	03-02b4	127 / 0 / 404 / 269 -0.68	259 / 0 / 990 / 261 -0.66	124 / 40 / 179 / 257 -0.56	157 / 40 / 127 / 76 -0.13
	03-02b5	405 / 0 / 451 / 73 -0.13	551 / 0 / 573 / 73 -0.08	373 / 75 / 368 / 365 -0.33	79 / 15 / 32 / 28 0.14
	03-02b6	167 / 0 / 221 / 62 -0.26	133 / 0 / 178 / 12 -0.18	169 / 60 / 257 / 631 -0.68	16 / 5 / 7 / 5 0.14
	Mean Sup/Inf ± SEM	222 ± 70/388 ± 120 -0.27 ± 0.15	277 ± 90/485 ± 239 -0.27 ± 0.16	165 ± 63/564 ± 134 -0.55 ± 0.09	100 ± 42/110 ± 51 -0.05 ± 0.06
S1	1	58 / 0 / 217 / 38 -0.63	128 / 0 / 440 / 6 -0.55	17 / 5 / 84 / 137 -0.86	32 / 5 / 23 / 17 -0.11
Enu	2	31 / 0 / 73 / 20 -0.50	88 / 0 / 240 / 11 -0.48	40 / 8 / 180 / 153 -0.79	144 / 13 / 48 / 73 0.09

3	94 / 0 / 194 / 40 -0.43	151 / 0 / 452 / 14 -0.51	15 / 8 / 75 / 122 -0.86	12 / 3 / 19 / 18 -0.51
4	47 / 0 / 101 / 10 -0.41	178 / 0 / 415 / 7 -0.41	53 / 38 / 123 / 173 -0.70	119 / 6 / 42 / 73 0.02
5	44 / 0 / 62 / 9 -0.24	275 / 0 / 256 / 4 0.28	39 / 25 / 161 / 184 -0.80	108 / 16 / 34 / 58 0.08
Mean Sup/Inf ± SEM	55 ± 12/153 ± 43 -0.47 ± 0.07	164 ± 35/369 ± 54 -0.39 ± 0.12	33 ± 8/278 ± 36 -0.79 ± 0.03	83 ± 29/81 ± 20 0.01 ± 0.13

TABLE 4: Stereological sampling parameters for the estimation of the number of anterogradely labeled axonal swellings in each layers in S1BF after injections of BDA into V1 of intact C57Bl/6 mice.

Case	Layer	Number of sections	Total area (mm^2)	Number of dissectors	Number of objects	Sampling fraction	Total estimation	CE
1	I-III	9	8661	106	313	0.004	84662	0.060
	IV	9	5663	117	164	0.006	26279	0.053
	Va	9	3150	117	178	0.011	15865	0.065
	Vbc	9	5407	115	164	0.006	25527	0.050
	VI	9	3950	116	78	0.009	8793	0.097
	Total (Mean)	45	26831	571	897	(0.007)	161126	(0.065)
2	I-III	9	6593	112	329	0.005	64112	0.074
	IV	9	4580	111	118	0.007	16117	0.075
	Va	9	2257	128	139	0.017	8115	0.074
	Vbc	9	3969	119	129	0.009	14243	0.089
	VI	9	2050	111	80	0.016	4890	0.083
	Total (Mean)	45	19449	581	795	(0.011)	107477	(0.079)
3	I-III	9	17372	110	317	0.002	165717	0.075
	IV	9	11941	112	158	0.003	55764	0.052
	Va	9	6617	127	181	0.006	31218	0.060
	Vbc	9	10180	123	156	0.004	42739	0.051
	VI	9	10885	64	111	0.003	20776	0.063
	Total (Mean)	45	56995	536	923	(0.004)	316214	(0.060)
4	I-III	5	2507	106	174	0.013	13519	0.194
	IV	5	1521	105	72	0.021	3427	0.201
	Va	5	940	114	60	0.037	1626	0.192
	Vbc	5	1408	110	90	0.024	3786	0.147
	VI	5	1515	105	141	0.021	6685	0.167
	Total (Mean)	25	7891	540	537	(0.023)	29043	(0.180)
5	I-III	10	5745	118	97	0.006	17793	0.071
	IV	10	3005	105	38	0.009	4097	0.097
	Va	10	1821	120	63	0.018	3602	0.044
	Vbc	10	2506	115	42	0.012	3449	0.052
	VI	10	1398	112	40	0.021	1881	0.070
	Total (Mean)	50	14475	570	280	(0.013)	30822	(0.067)

TABLE 5: Stereological sampling parameters for the estimation of the number of anterogradely labeled axonal swellings in each layers in S1BF after injections of BDA into V1 of enucleated C57Bl/6 mice.

Case	Layer	Number of sections	Total area (mm^2)	Number of dissectors	Number of objects	Sampling fraction	Total estimation	CE
IC-01	I-III	10	7596	111	106	0.009	23344	0.076
	IV	10	5712	117	100	0.010	15712	0.079
	Va	10	3582	119	99	0.010	9590	0.070
	Vbc	10	6726	114	119	0.008	22596	0.071
	VI	10	5632	113	74	0.014	11869	0.085
	Total (Mean)	50	29248	574	498	(0.010)	83111	(0.076)
IC-02	I-III	11	9185	125	103	0.010	27566	0.087
	IV	11	6728	123	40	0.025	7968	0.078
	Va	11	3230	142	45	0.022	3729	0.093
	Vbc	11	5141	138	70	0.014	9483	0.078
	VI	11	6582	119	99	0.010	19945	0.089
	Total (Mean)	55	30866	647	357	(0.016)	68691	(0.085)
IC-03	I-III	10	1382	144	167	0.006	5161	0.063
	IV	10	1534	139	85	0.012	3020	0.081
	Va	10	1020	133	119	0.008	2937	0.068
	Vbc	10	1922	125	73	0.014	3613	0.102
	VI	10	2375	122	134	0.008	8395	0.106
	Total (Mean)	50	8233	663	578	(0.010)	23126	(0.084)
IC-04	I-III	10	10264	109	232	0.004	70308	0.046
	IV	10	4180	135	233	0.004	23213	0.045
	Va	10	2840	143	233	0.004	14896	0.036
	Vbc	10	5188	127	220	0.005	28920	0.053
	VI	10	6240	114	229	0.004	40346	0.048
	Total (Mean)	50	28712	628	1147	(0.004)	177683	(0.046)
IC-05	I-III	10	1615	106	247	0.004	13688	0.042
	IV	10	780	123	148	0.007	3432	0.055
	Va	10	472	130	123	0.008	1597	0.059
	Vbc	10	611	121	87	0.012	1580	0.071
	VI	10	577	119	46	0.022	801	0.077
	Total (Mean)	50	4055	599	651	(0.011)	21098	(0.061)

TABLE 6: Stereological sampling parameters for the estimation of the number of anterogradely labeled axonal swellings in each layers in V1 after injections of BDA into S1BF of intact C57Bl/6 mice.

Case	Layer	Number of sections	Total area (mm^2)	Number of dissectors	Number of objects	Sampling fraction	Total estimation	CE
1	I-III	11	9174	124	201	0.004	53794	0.089
	IV	11	6717	122	80	0.005	15935	0.078
	Va	11	3229	141	85	0.012	7043	0.098
	Vbc	11	5130	137	137	0.007	18558	0.085
	VI	11	6571	118	194	0.005	39083	0.090
	Total (Mean)	55	30821	642	697	(0.007)	134413	(0.088)
2	I-III	10	1604	105	488	0.018	27043	0.043
	IV	10	779	122	291	0.043	6747	0.056
	Va	10	461	129	241	0.077	3129	0.059
	Vbc	10	600	120	169	0.055	3070	0.072
	VI	10	566	118	89	0.058	1549	0.082
	Total (Mean)	50	4010	594	1278	(0.050)	41538	(0.062)
3	I-III	10	1380	108	209	0.022	9692	0.061
	IV	10	578	119	153	0.057	2696	0.050
	Va	10	461	124	146	0.074	1971	0.061
	Vbc	10	649	128	128	0.054	2355	0.057
	VI	10	607	153	91	0.070	1310	0.059
	Total (Mean)	50	3675	632	727	(0.055)	18024	(0.058)
4	I-III	7	3414	111	254	0.010	25597	0.080
	IV	7	1343	133	106	0.030	3508	0.092
	Va	7	819	115	90	0.043	2102	0.099
	Vbc	7	1317	105	65	0.024	2671	0.094
	VI	7	1295	124	64	0.029	2190	0.093
	Total (Mean)	35	8188	588	579	(0.027)	36068	(0.092)
5	I-III	8	1493	121	152	0.025	6192	0.052
	IV	8	709	139	82	0.059	1381	0.040
	Va	8	403	158	56	0.119	472	0.068
	Vbc	8	710	138	52	0.059	883	0.069
	VI	8	678	134	50	0.060	835	0.026
	Total (Mean)	40	3993	690	392	(0.064)	9763	(0.051)

TABLE 7: Stereological sampling parameters for the estimation of the number of anterogradely labeled axonal swellings in each layers in V1 after injections of BDA into S1BF of enucleated C57Bl/6 mice.

Case	Layer	Number of sections	Total area (mm^2)	Number of dissectors	Number of objects	Sampling fraction	Total estimation	CE
IC-06	I-III	10	3284	116	36	0.028	3697	0.060
	IV	10	1448	130	32	0.031	1293	0.054
	Va	10	982	142	26	0.039	652	0.057
	Vbc	10	1471	125	26	0.039	1110	0.080
	VI	10	1875	116	18	0.056	1056	0.052
	Total (Mean)	50	9060	629	138	(0.039)	7808	(0.061)
IC-07	I-III	10	8722	123	59	0.017	15177	0.069
	IV	10	3326	135	52	0.019	4647	0.073
	Va	10	1919	139	39	0.026	1954	0.083
	Vbc	10	3572	123	46	0.022	4846	0.085
	VI	10	3974	127	49	0.020	5562	0.058
	Total (Mean)	50	21513	647	245	(0.021)	32186	(0.074)
IC-08	I-III	10	1391	109	21	0.048	974	0.067
	IV	10	589	120	14	0.071	247	0.083
	Va	10	472	125	15	0.067	203	0.072
	Vbc	10	650	129	14	0.071	258	0.098
	VI	10	618	154	9	0.111	130	0.094
	Total (Mean)	50	3720	637	73	(0.074)	1812	(0.083)
IC-09	I-III	10	4451	112	66	0.015	9516	0.056
	IV	10	1901	124	54	0.019	3003	0.056
	Va	10	1017	145	65	0.015	1654	0.047
	Vbc	10	2090	111	65	0.015	4440	0.042
	VI	10	1017	118	57	0.018	1782	0.063
	Total (Mean)	50	10476	610	307	(0.016)	20395	(0.053)
IC-10	I-III	8	3102	110	47	0.021	4879	0.087
	IV	8	1242	128	42	0.024	1501	0.067
	Va	8	733	127	33	0.030	701	0.102
	Vbc	8	1249	129	35	0.029	1247	0.082
	VI	8	1429	122	26	0.038	1121	0.123
	Total (Mean)	40	7755	616	183	0.028	9449	0.092

TABLE 8: Sampling parameters for the estimation of the diameter of anterogradely labeled axons as they enter the gray matter in S1BF and V1 after injections of BDA into V1 and S1BF respectively of intact and enucleated at birth C57Bl/6 mice.

Injection site	Group	Case	Number of sections	Sampled length (mm)	Number of axons
V1	Intact	1	9	13.281	259
		2	9	12.215	116
		3	9	14.372	104
		4	5	6.567	195
		5	10	13.967	132
V1	Enucleated	1	10	18.845	213
		2	11	11.763	117
		3	10	17.524	52
		4	10	14.467	326
		5	10	8.171	48
S1BF	Intact	1	11	11.532	134
		2	10	6.016	38
		3	10	5.373	154
		4	7	6.215	84
		5	8	6.143	310
S1BF	Enucleated	1	10	13.135	25
		2	10	13.314	83
		3	10	10.489	3
		4	10	15.750	42
		5	8	8.312	19

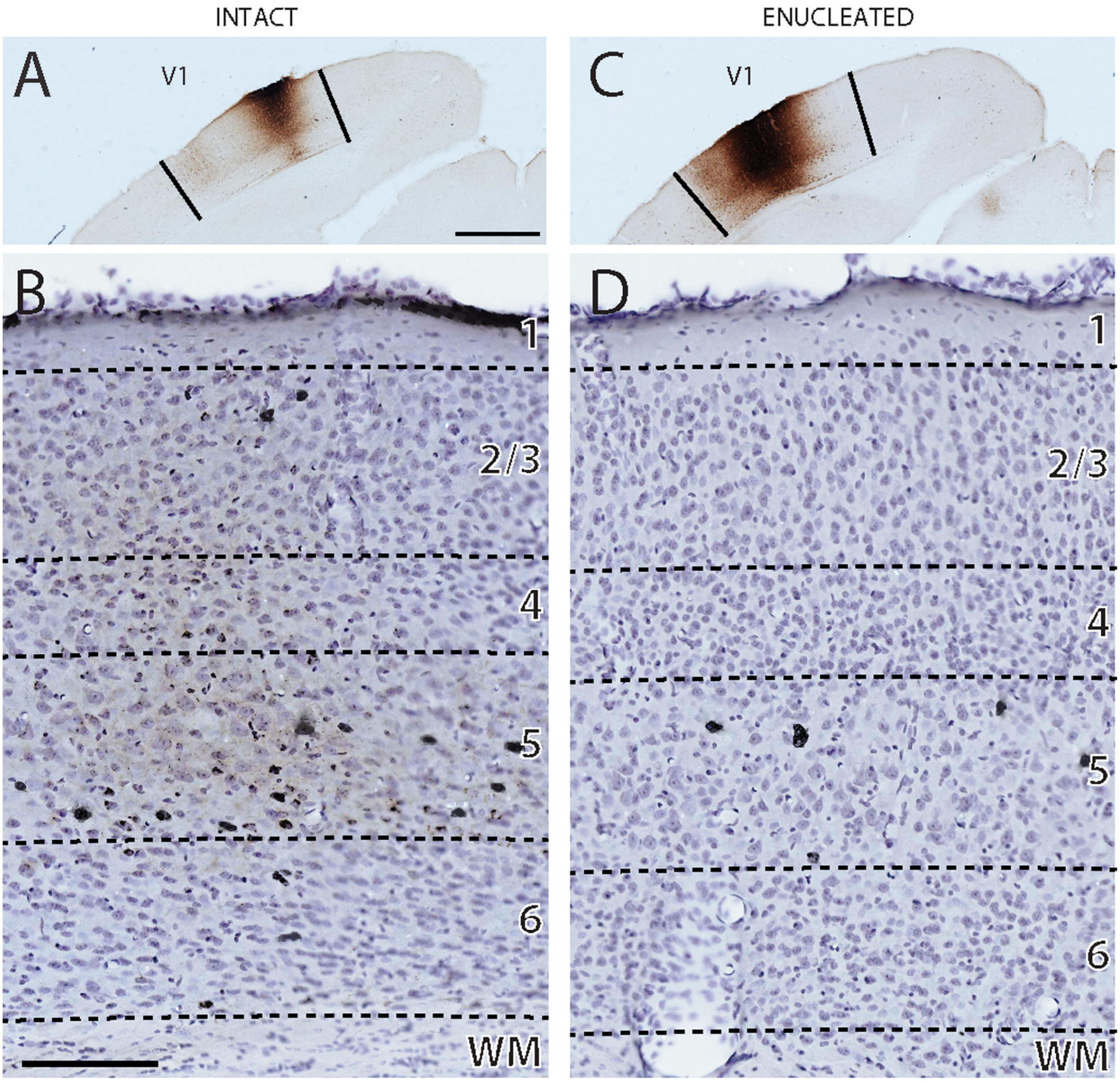
INTACT
ENUCLEATED
A
V1
C
V1
B
1
2/3
4
5
6
WM
D
1
2/3
4
5
6
WM

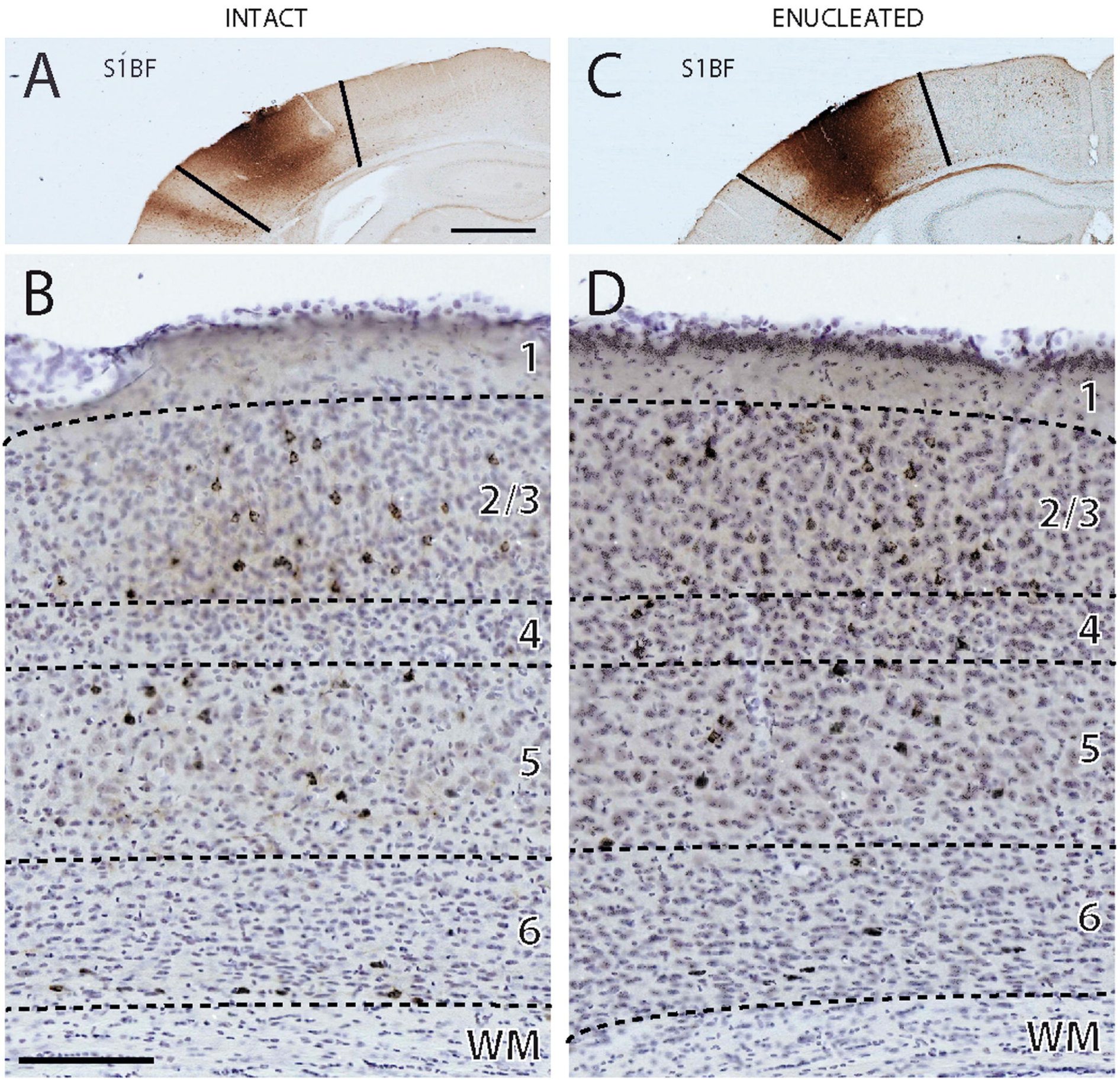
INTACT
ENUCLEATED
A
S1BF
C
S1BF
B
1
2/3
4
5
6
WM
D
1
2/3
4
5
6
WM

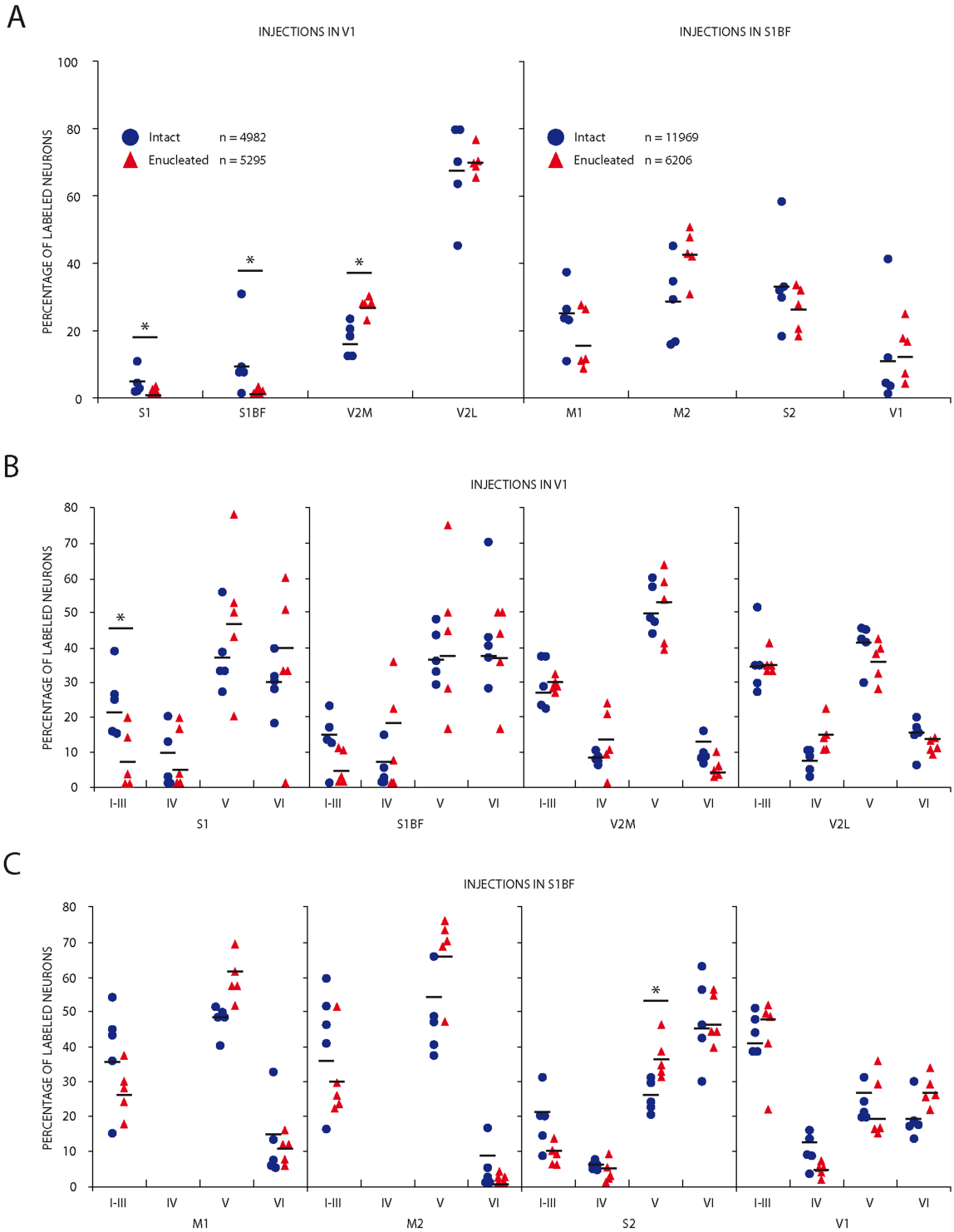
A
INJECTIONS IN V1
INJECTIONS IN S1BF
PERCENTAGE OF LABELED NEURONS
Intact n = 4982
Enucleated n = 5295
Intact n = 11969
Enucleated n = 6206
S1
S1BF
V2M
V2L
M1
M2
S2
V1
B
INJECTIONS IN V1
I-III
IV
V
VI
C
INJECTIONS IN S1BF

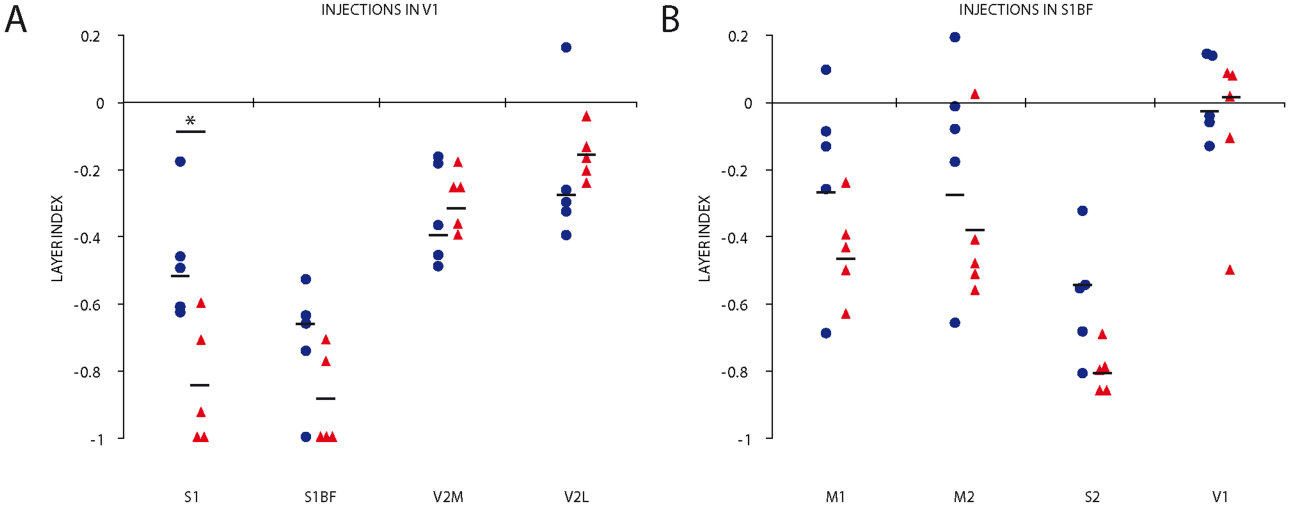
A
INJECTIONS IN V1
LAYER INDEX
0.2
0
-0.2
-0.4
-0.6
-0.8
-1
*
S1
S1BF
V2M
V2L
B
INJECTIONS IN S1BF
LAYER INDEX
0.2
0
-0.2
-0.4
-0.6
-0.8
-1
M1
M2
S2
V1

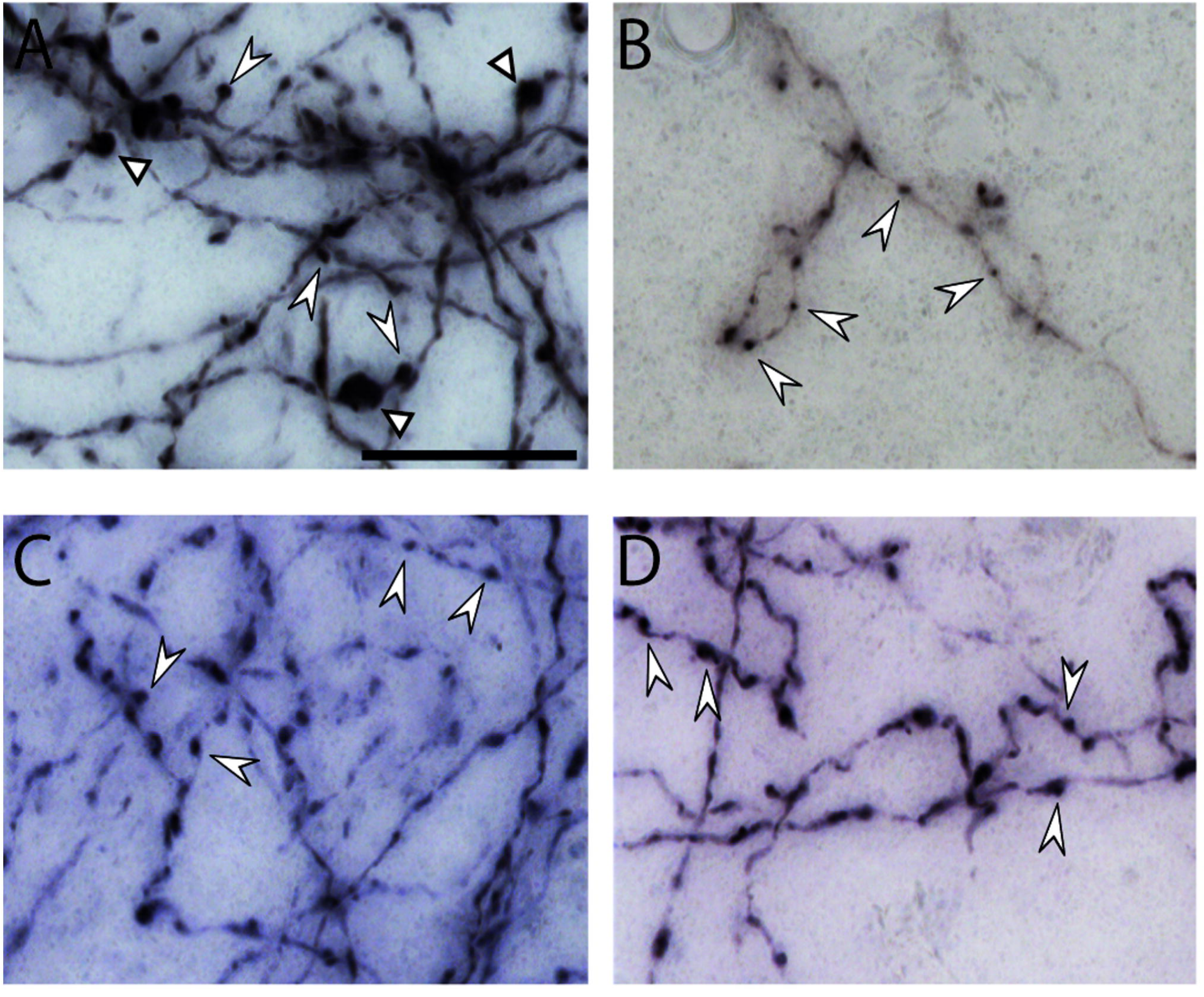
A
B
C
D

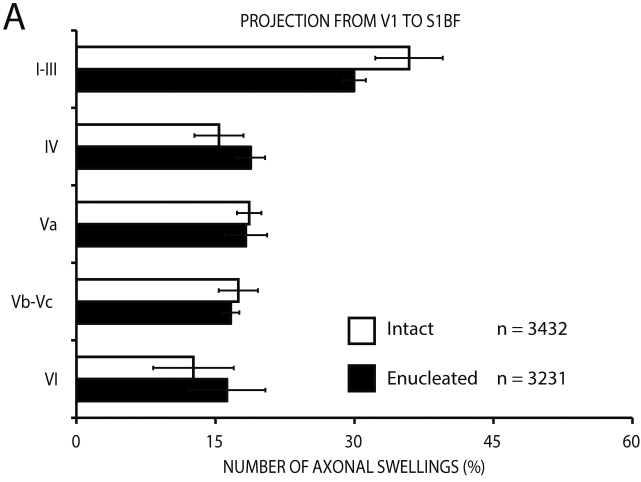
A
PROJECTION FROM V1 TO S1BF
I-III
IV
Va
Vb-Vc
VI
Intact
n = 3432
Enucleated
n = 3231
0
15
30
45
60
NUMBER OF AXONAL SWELLINGS (%)

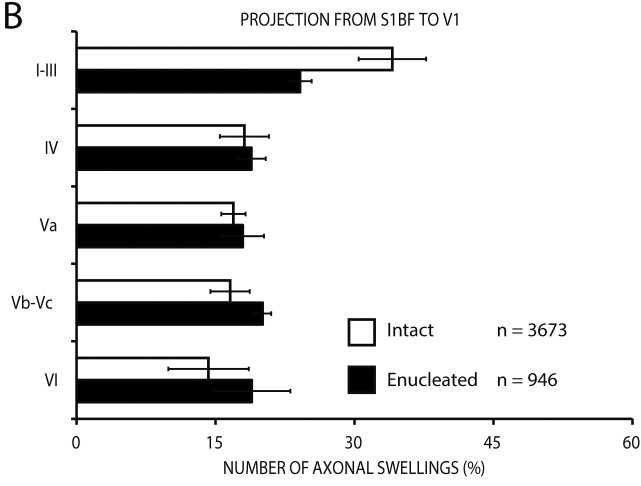
B
PROJECTION FROM S1BF TO V1
I-III
IV
Va
Vb-Vc
VI
Intact
n = 3673
Enucleated
n = 946
0
15
30
45
60
NUMBER OF AXONAL SWELLINGS (%)

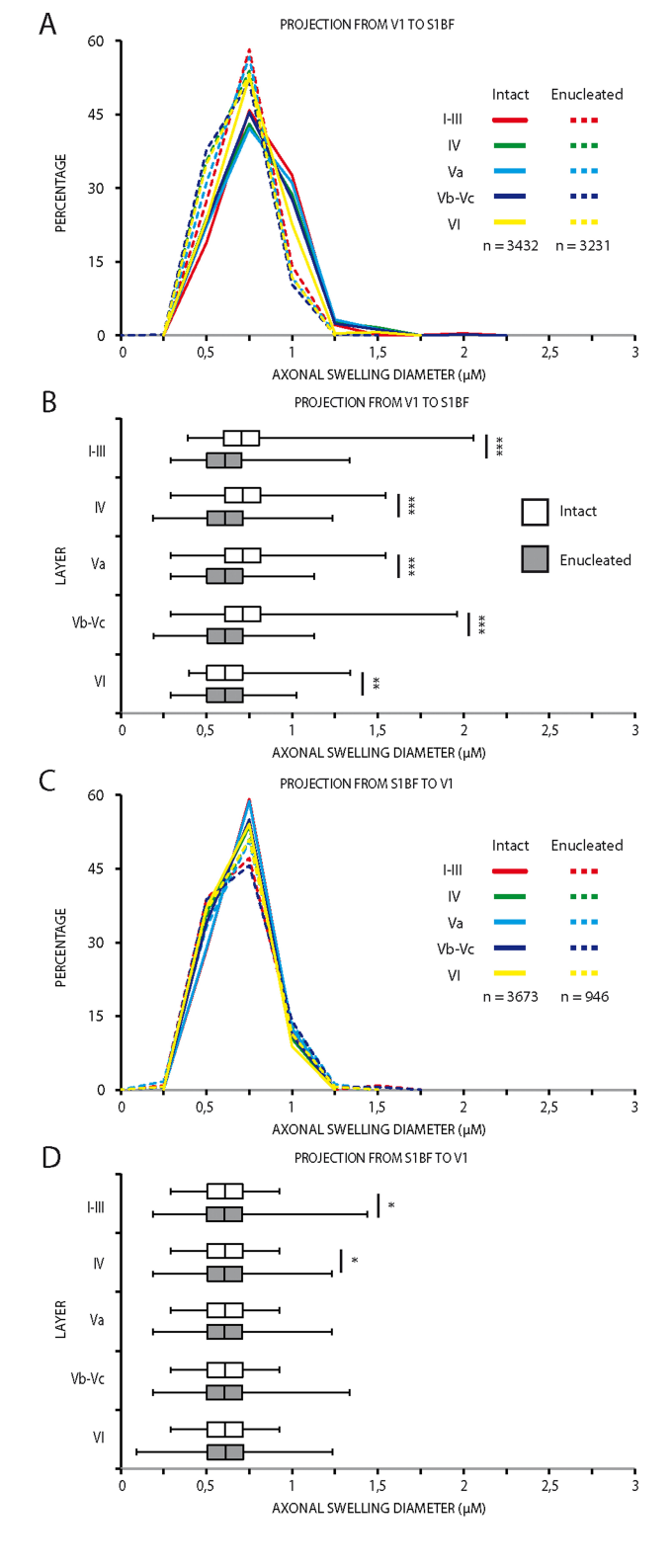
A
PROJECTION FROM V1 TO S1BF
PERCENTAGE
AXONAL SWELLING DIAMETER (µM)
Intact
Enucleated
I-III
IV
Va
Vb-Vc
VI
n = 3432
n = 3231
B
PROJECTION FROM V1 TO S1BF
LAYER
AXONAL SWELLING DIAMETER (µM)
Intact
Enucleated
C
PROJECTION FROM S1BF TO V1
PERCENTAGE
AXONAL SWELLING DIAMETER (µM)
Intact
Enucleated
n = 3673
n = 946
D
PROJECTION FROM S1BF TO V1
LAYER
AXONAL SWELLING DIAMETER (µM)

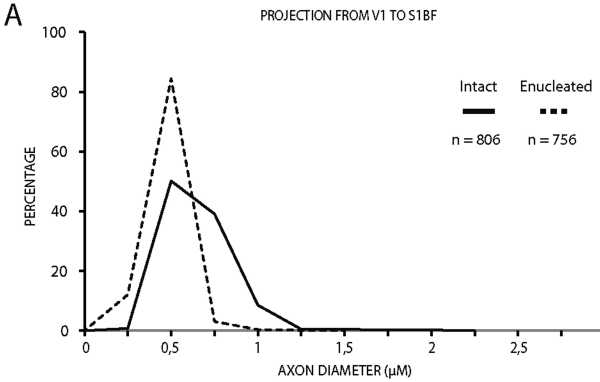
A
PROJECTION FROM V1 TO S1BF
Intact
Enucleated
n = 806
n = 756
PERCENTAGE
AXON DIAMETER (µM)
0
20
40
60
80
100
0
0,5
1
1,5
2
2,5
3

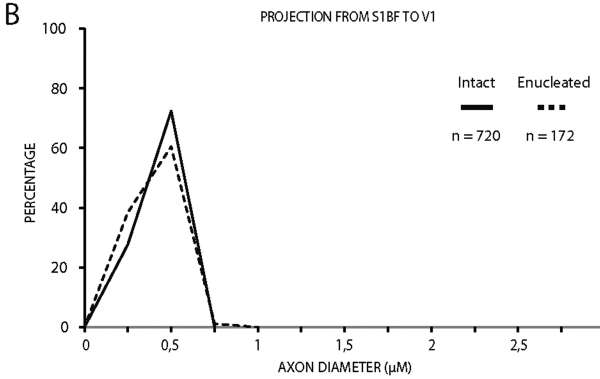
B
PROJECTION FROM S1BF TO V1
Intact
Enucleated
n = 720
n = 172
PERCENTAGE
AXON DIAMETER (µM)
0
20
40
60
80
100
0
0,5
1
1,5
2
2,5
3

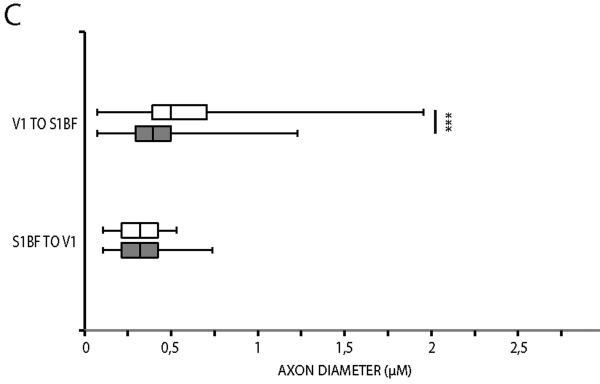
C
V1 TO S1BF
S1BF TO V1
***
AXON DIAMETER (µM)
0
0,5
1
1,5
2
2,5
3